Turbulence control on a NACA 4412 wing section assessed through high-fidelity simulations

Fermín Mallor, **Marco Atzori, Alvaro Tanarro,**

Nicolas Offermans, Adam Peplinski,

Ricardo Vinuesa & Philipp Schlatter

Linné FLOW Centre and

Swedish e-Science Research Centre (SeRC)

KTH Mechanics, Stockholm, Sweden

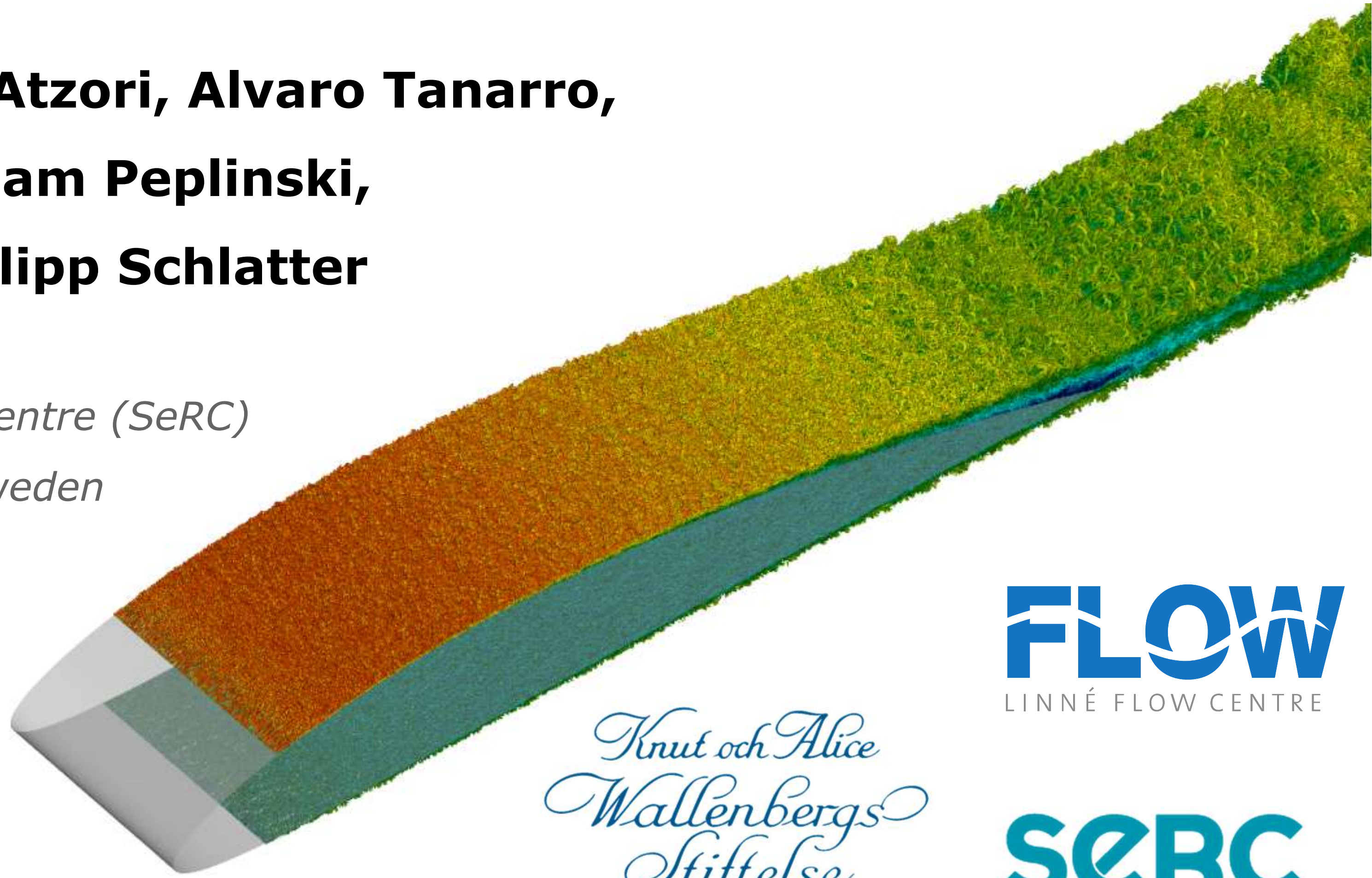

FLOW
LINNÉ FLOW CENTRE

Knut och Alice Wallenbergs Stiftelse

SeRC
Swedish e-Science Research Centre

KTH VETENSKAP OCH KONST

Aerospace Technology Congress, Stockholm, 8 October 2019

Outline

- Introduction
- Flow control on a NACA 4412 wing
  - Effects on the flow
  - Aerodynamic effects
- Enabling high Re well-resolved simulations
  - LES RT-filter
  - Adaptive Mesh Refinement
- Experimental campaign
- Conclusions

Why CFD?

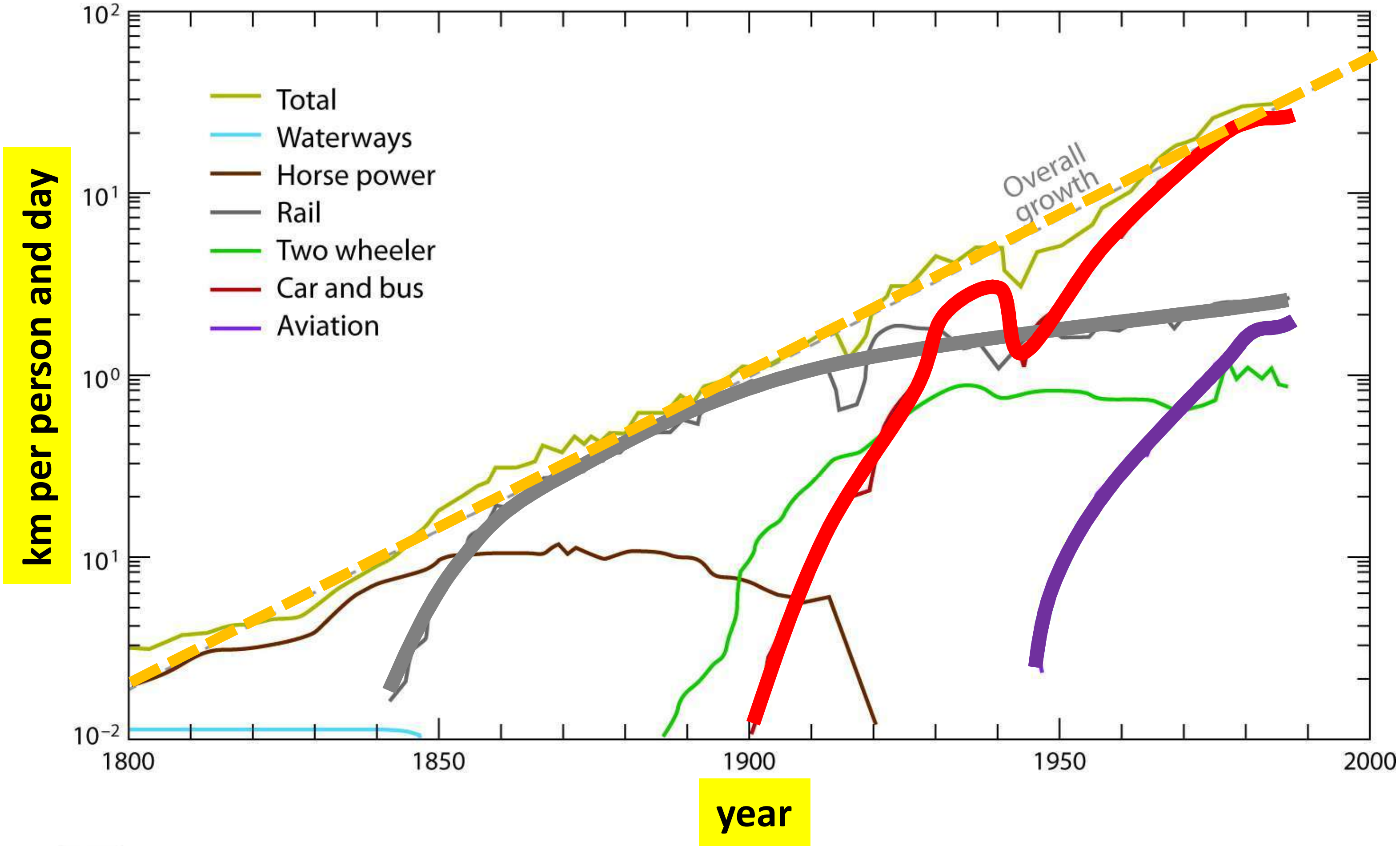

Banister D, et al. 2011.
Annu Rev. Environ. Resour. 36:247–70

Source:
[1] www.bombardier.com

Why CFD?

Skin friction/drag reduction is the key for economically and ecologically more efficient transport

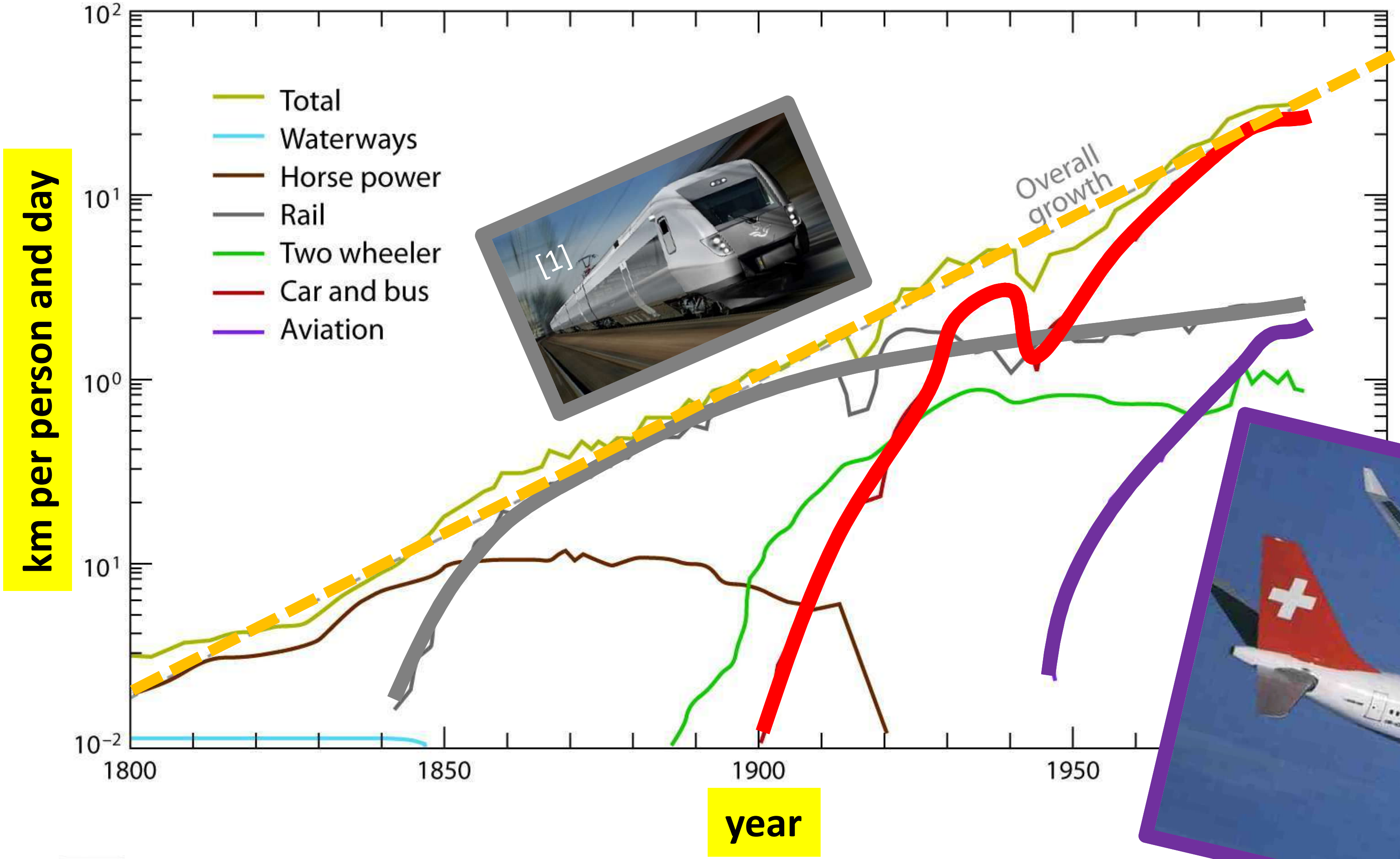

Banister D, et al. 2011.
Annu Rev. Environ. Resour. 36:247–70

Source:
[1] www.bombardier.com

Study case: NACA 4412, $Re_c = 200,000$

NACA 4412:
Maximum camber of 4% at 40% chord with a maximum thickness of 12%

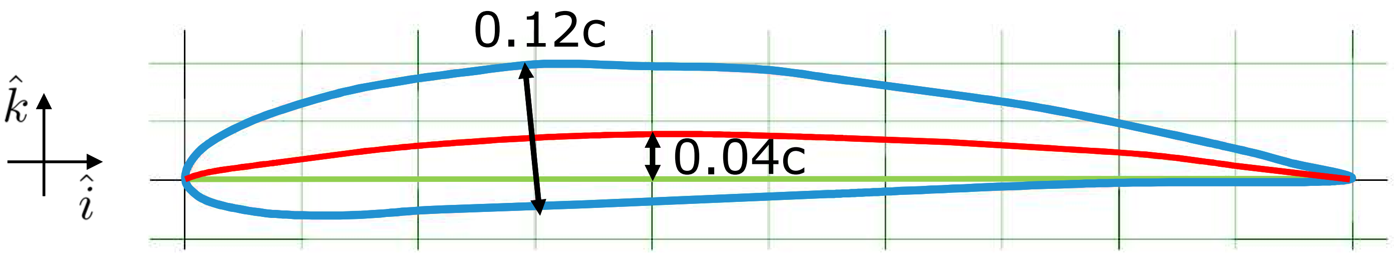

$$C_L = \frac{F_L}{qA} = \frac{F_L}{(\frac{1}{2}\rho U_\infty^2)A} = \frac{2}{\rho U_\infty^2 A}\int_A \tau_w(\hat{t}\cdot\hat{k})\mathrm{d}A + \frac{2}{\rho U_\infty^2 A}\int_A (p-p_0)(\hat{n}\cdot\hat{k})\mathrm{d}A$$

$$C_D = \frac{F_D}{qA} = \frac{F_D}{(\frac{1}{2}\rho U_\infty^2)A} = \underbrace{\frac{2}{\rho U_\infty^2 A}\int_A \tau_w(\hat{t}\cdot\hat{i})\mathrm{d}A}_{c_f} + \underbrace{\frac{2}{\rho U_\infty^2 A}\int_A (p-p_0)(\hat{n}\cdot\hat{i})\mathrm{d}A}_{c_p}$$

$$\rightarrow \boxed{\frac{L}{D}}$$

Friction drag **Pressure drag**

Numerical setup[1]

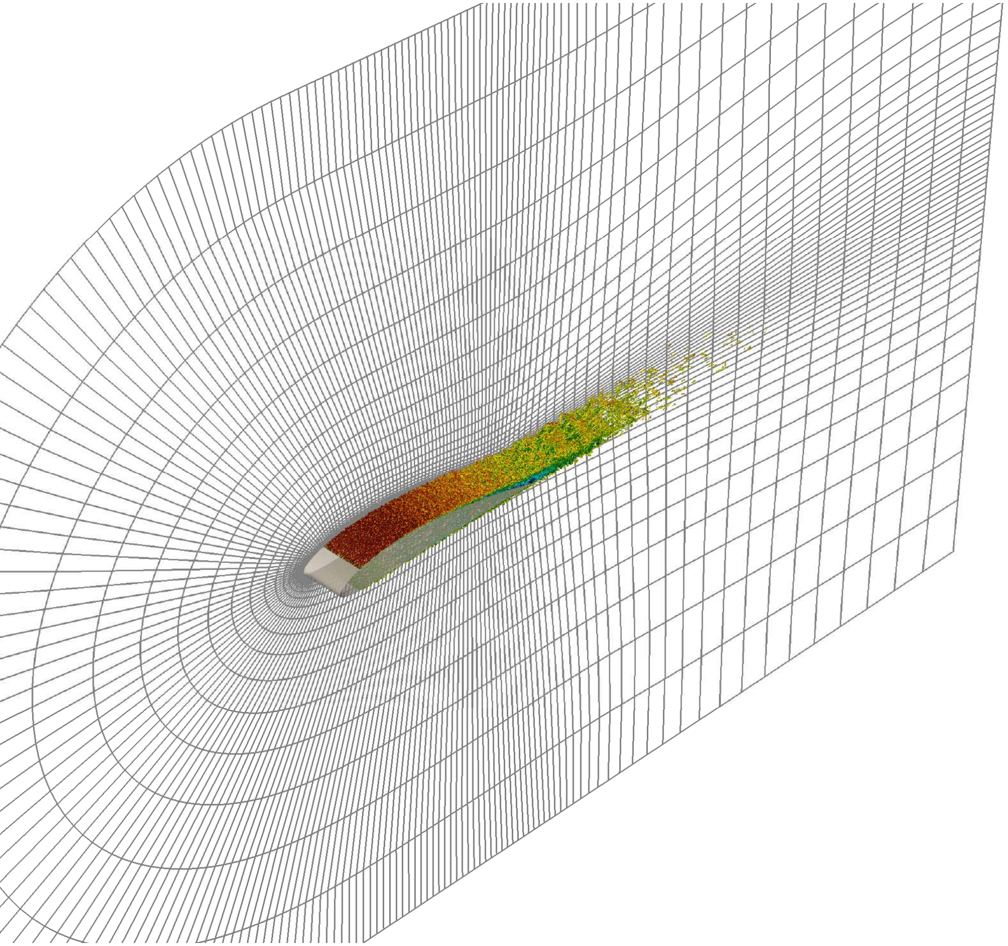

- Spectral-element code ***Nek5000***[2]
- 216 million grid points (N=11)
- 10 million core-hours
- Domain: $6c \times 4c \times 0.2c$
- Wall-resolved **LES**: $\Delta x^+ = 18$, $\Delta y^+ = (0.64, 11), \Delta z^+ = 9$
- **Time-resolved**
- LES using a relaxation-type filter model (Schlatter et al. 2005)
- **Tripping** at $x/c = 0.1c$

(1): Vinuesa *et al.*, Int. J. Heat Fluid Flow (2018), 72:86-99
(2): https://nek5000.mcs.anl.gov/, Fischer *et al.*, (2008)

Control strategies[1]

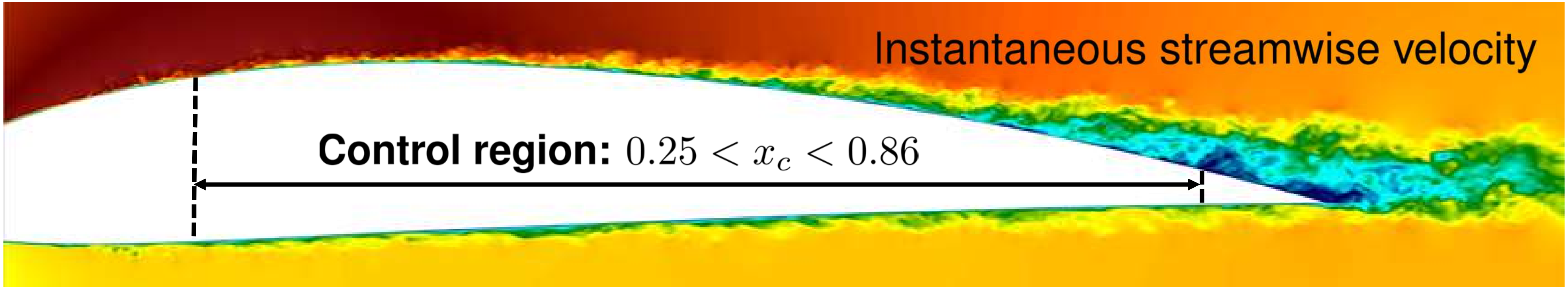

- **Suspion Side**
  - **Uniform Blowing**
    - 0.1% U∞ — 1
    - 0.2% U∞ — 2
  - **Uniform Suction**
    - 0.1% U∞ — 3
    - 0.2% U∞ — 4
- **Pressure Side**
  - **Uniform Blowing**
    - 0.1% U∞ — 5
    - 0.2% U∞ — 6
- **Suction Side** → **Body-force damping** → **As blowing, 0.1% U∞** — 7

(1) Atzori et al. DLES-12 2019

Effect of control

APG: $\uparrow U^+$

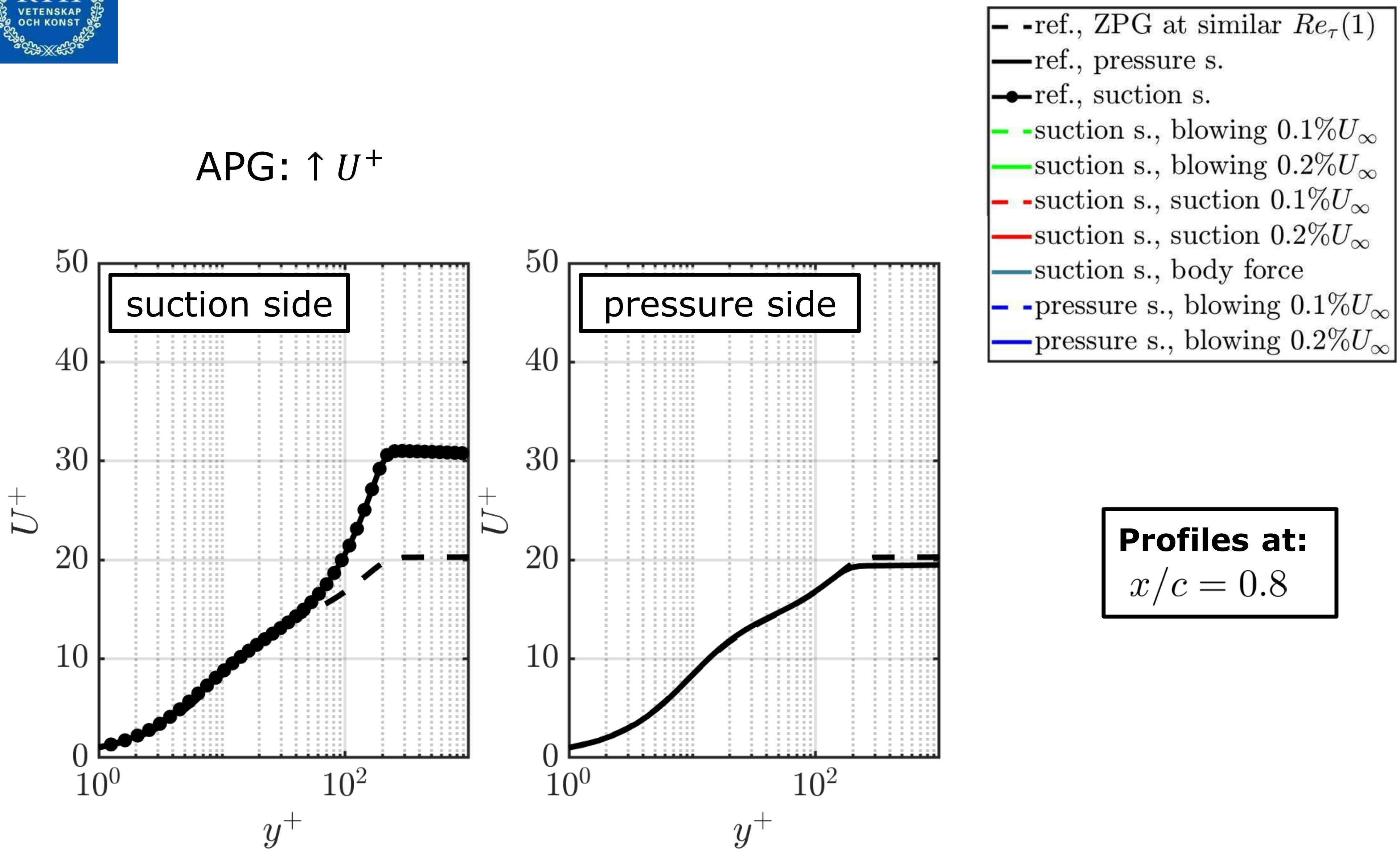

Profiles at:
$x/c = 0.8$

Effect of control

APG, blowing: $\uparrow U^+$

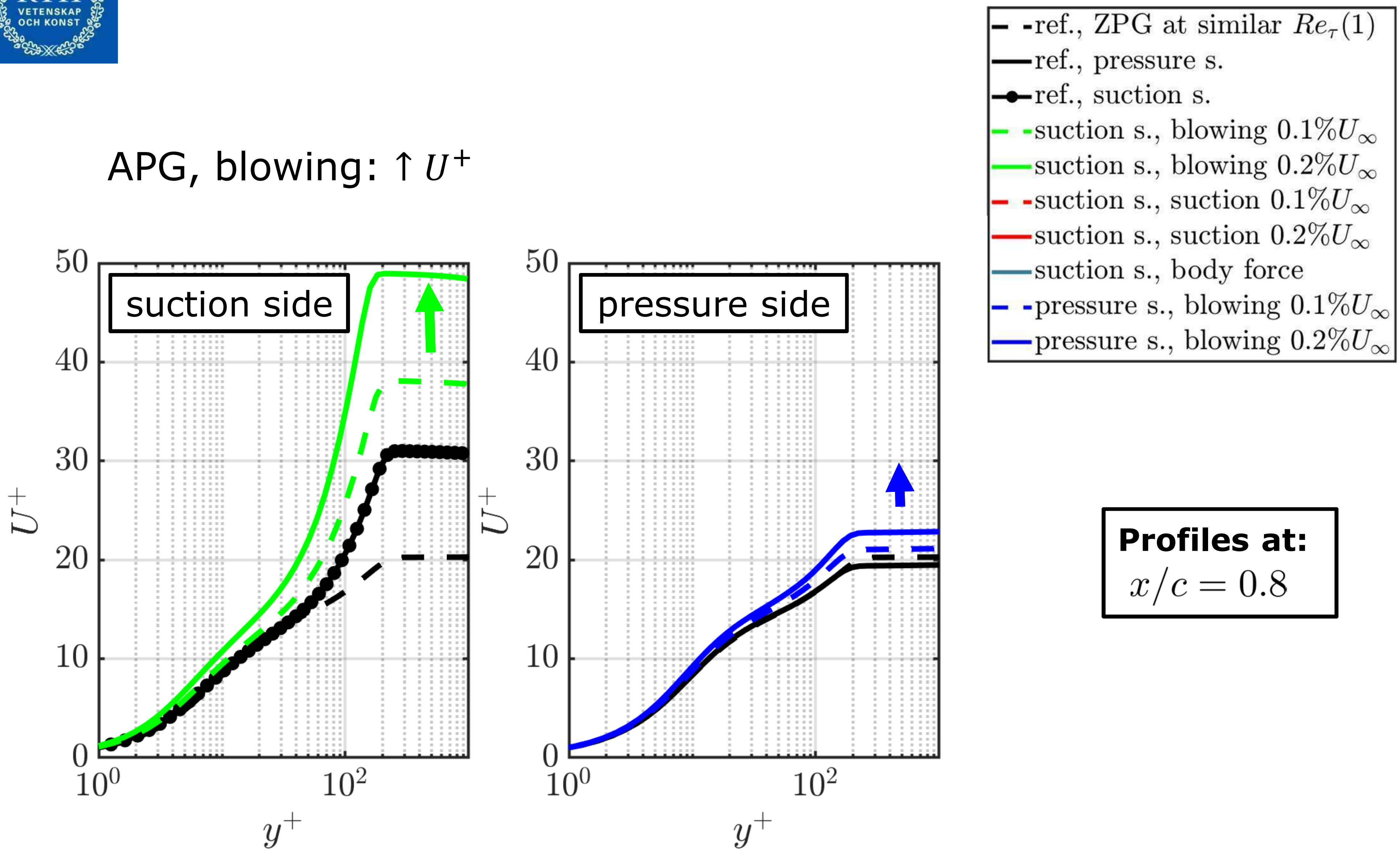

Profiles at:
$x/c = 0.8$

Effect of control

Suction: $\downarrow U^+$
APG, blowing: $\uparrow U^+$

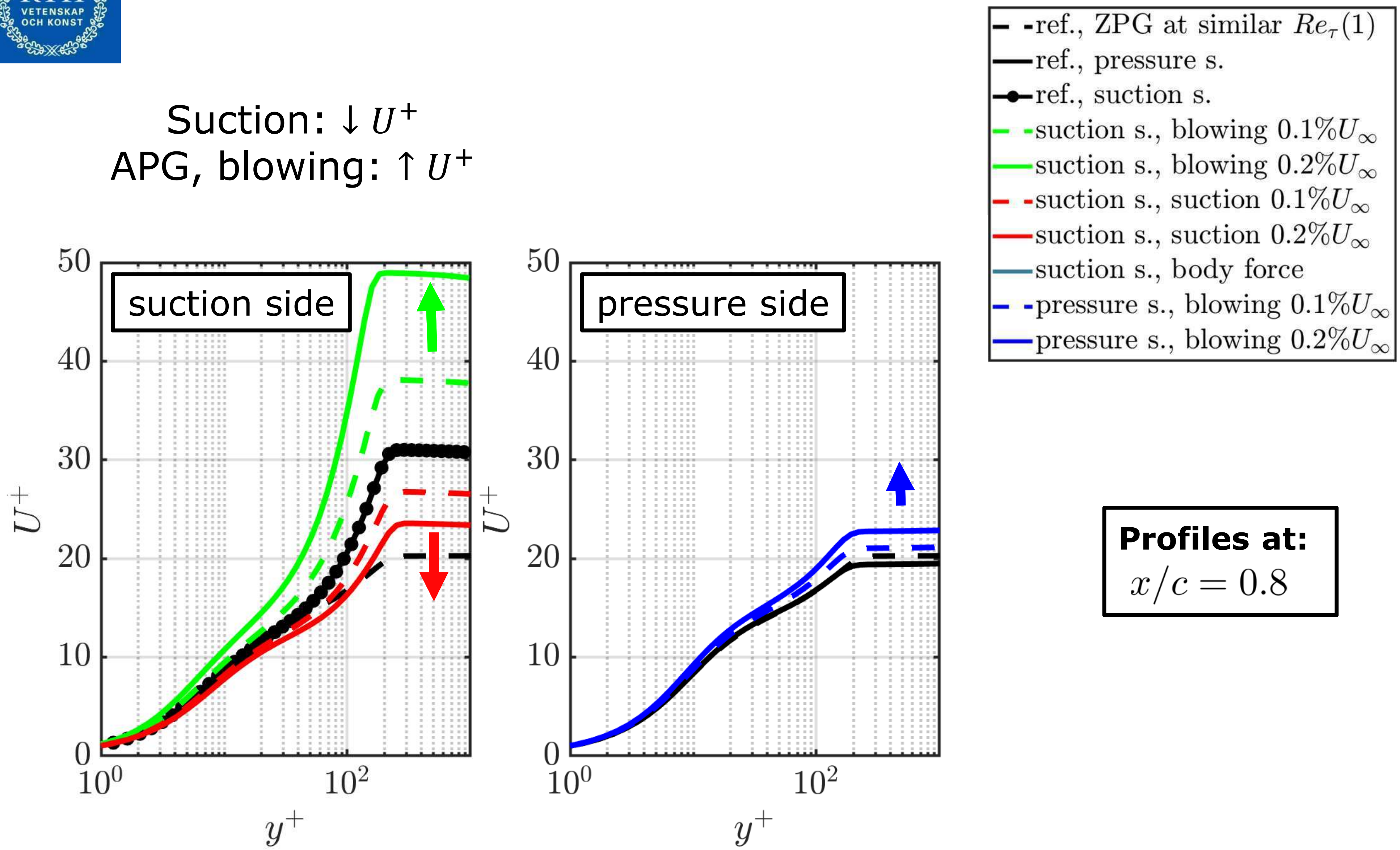

Profiles at:
$x/c = 0.8$

Effect of control

APG: ↓ C_f

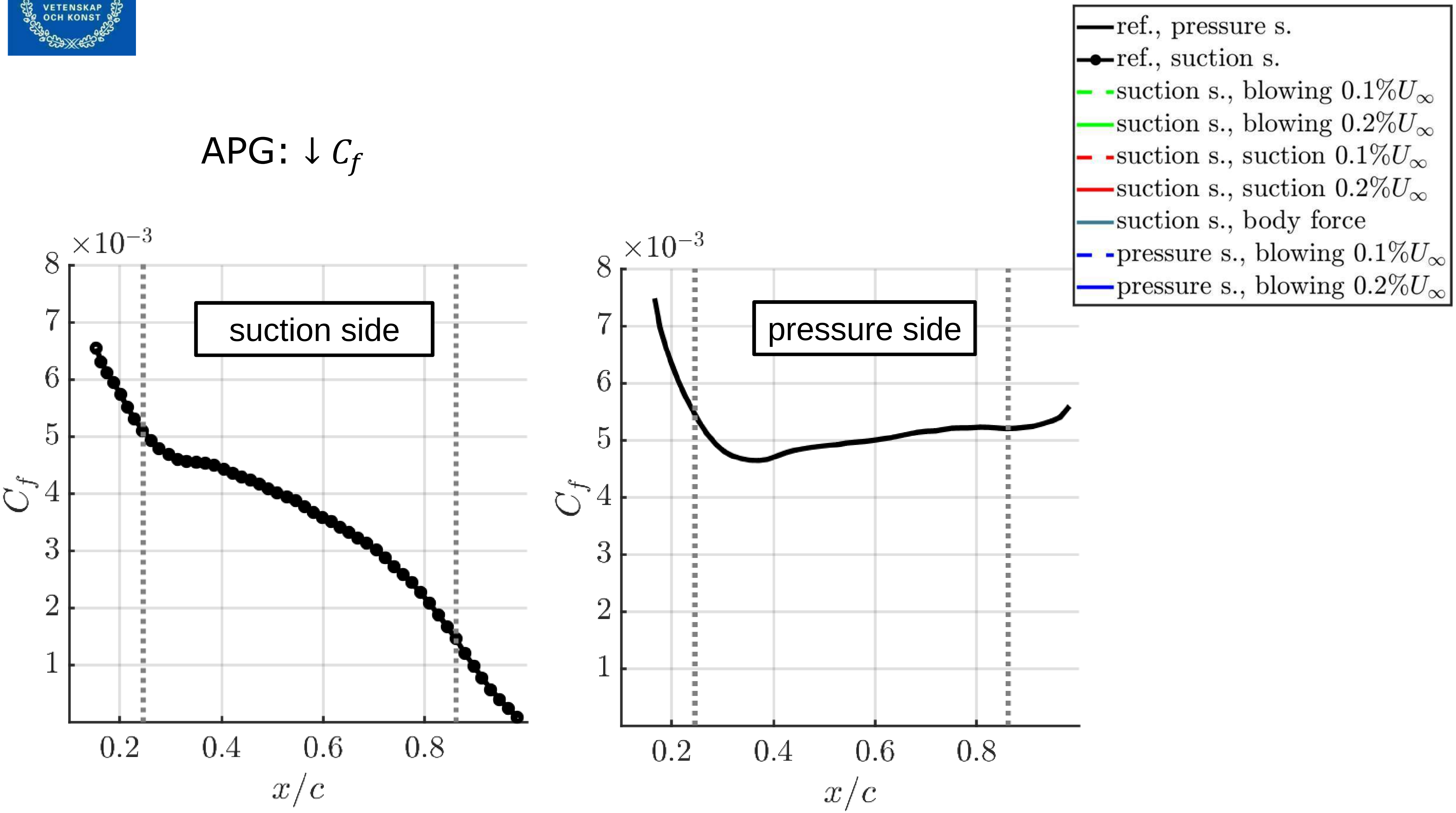

Effect of control

APG, blowing: $\downarrow C_f$

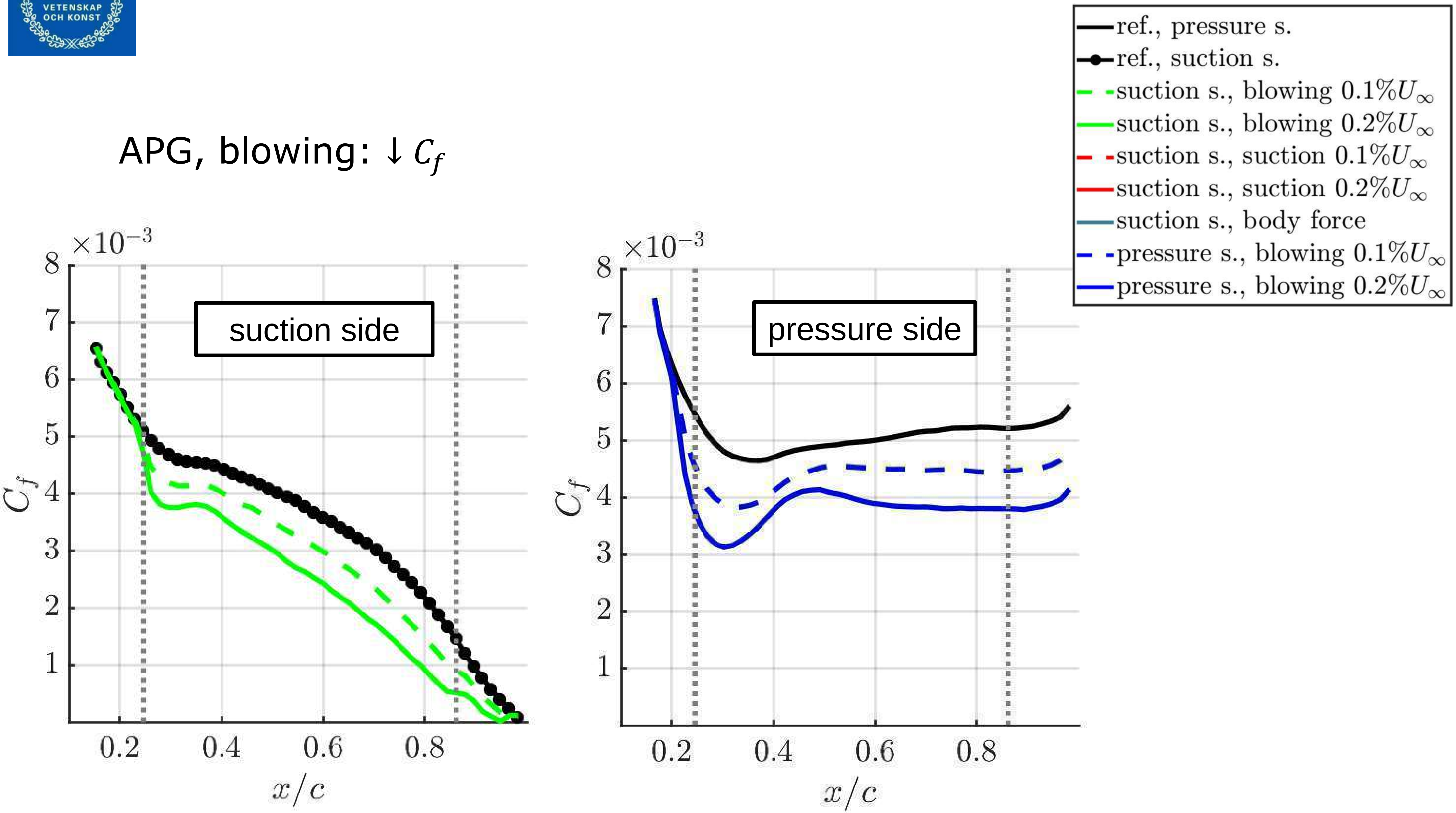

Effect of control

Suction: ↑ C_f
APG, blowing: ↓ C_f

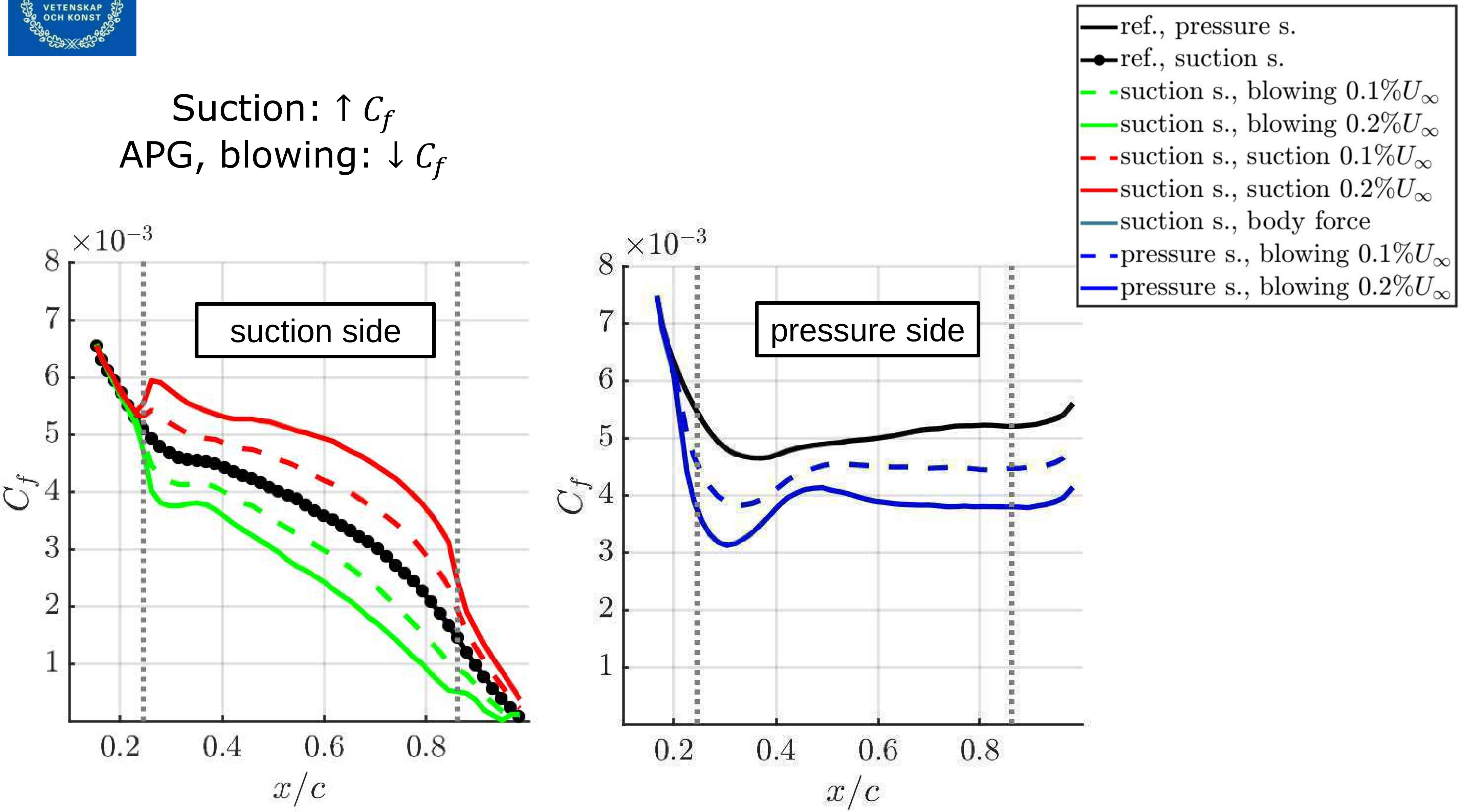

Friction drag (FIK) decomposition[1,2]

$$C_f(x) = C_f^\delta(x) + C_f^T(x) + C_f^D(x) + C_f^P(x)$$

B.L. thickness: $C_f^\delta = \dfrac{4(1-\delta_{99}/\delta^*)}{Re_\delta}$

Reynolds-shear stress: $C_f^T = 2\displaystyle\int_0^1 2(1-\eta)(-\overline{uv})\mathrm{d}\eta$

Streamwise development: $C_f^D = -2\displaystyle\int_0^1 (1-\eta)^2 I_x \mathrm{d}\eta$

Pressure: $C_f^P = -2\displaystyle\int_0^1 (1-\eta)^2 \frac{\partial P}{\partial x}\mathrm{d}\eta$

where:

$$\eta = \frac{y}{\delta_{99}}, \quad Re_\delta = \frac{U_e \delta_{99}}{\nu}, \quad I_x = \frac{\partial(U\,U)}{\partial x} + \frac{\partial \overline{uu}}{\partial x} + \frac{\partial(U\,V)}{\partial \eta} - \frac{1}{Re_\delta}\frac{\partial^2 U}{\partial x^2}$$

FLOW LINNÉ FLOW CENTRE

(1): Fukagata et al., Phys. Fluids (2002), 14:73-74
(2): Kametami et al., Int. J. Heat Fluid Flow (2015), 55:132-142

FIK: Boundary-layer thickness

$$C_f^{\delta} = \frac{4(1 - \delta_{99}/\delta^*)}{Re_\delta}$$

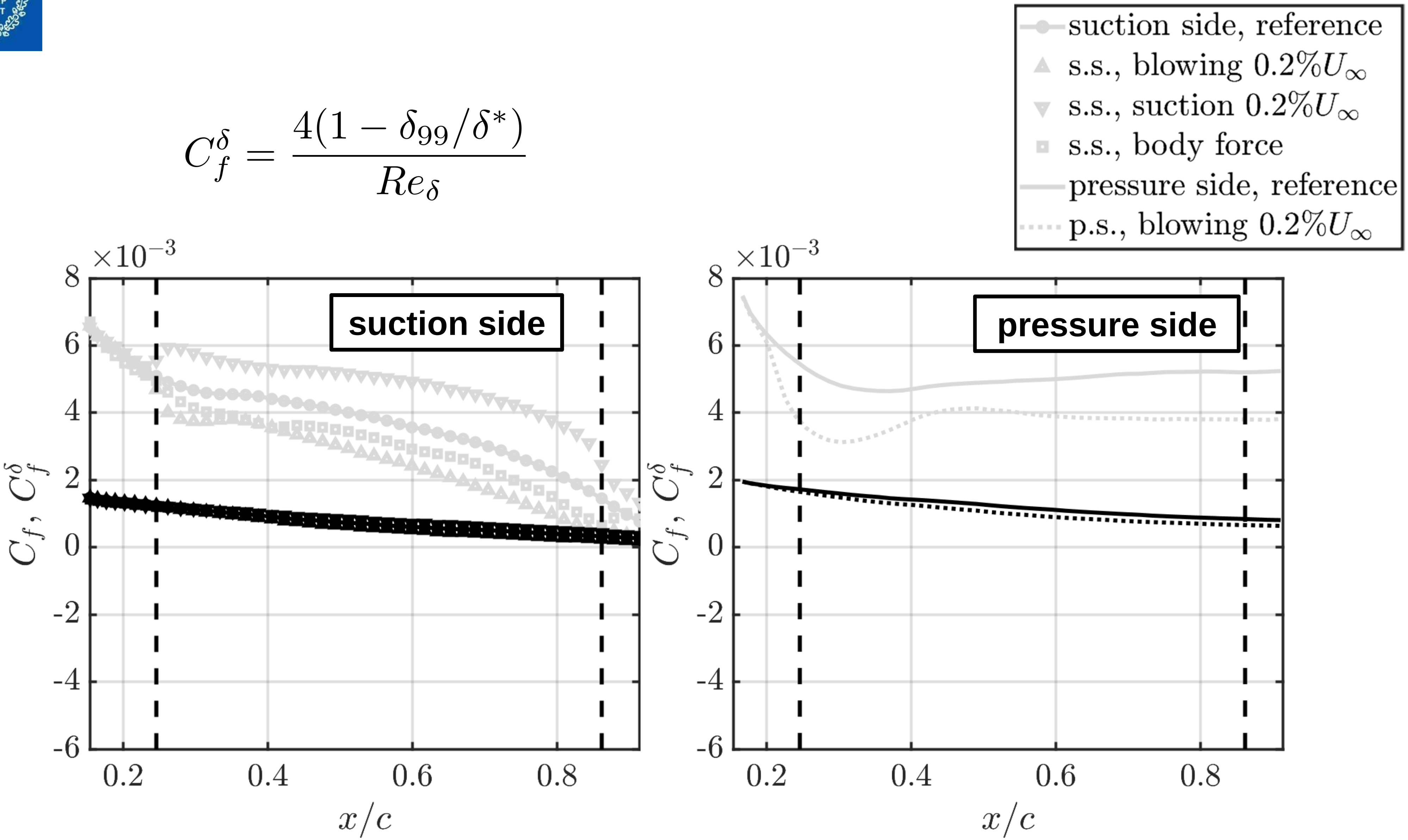

FIK: Turbulent fluctuations

$$C_f^T = 2\int_0^1 2(1-\eta)(-\overline{uv})\mathrm{d}\eta$$

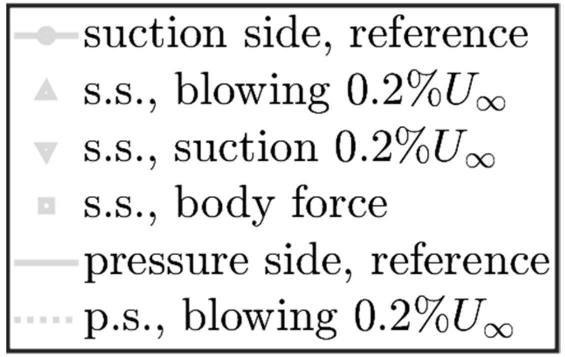

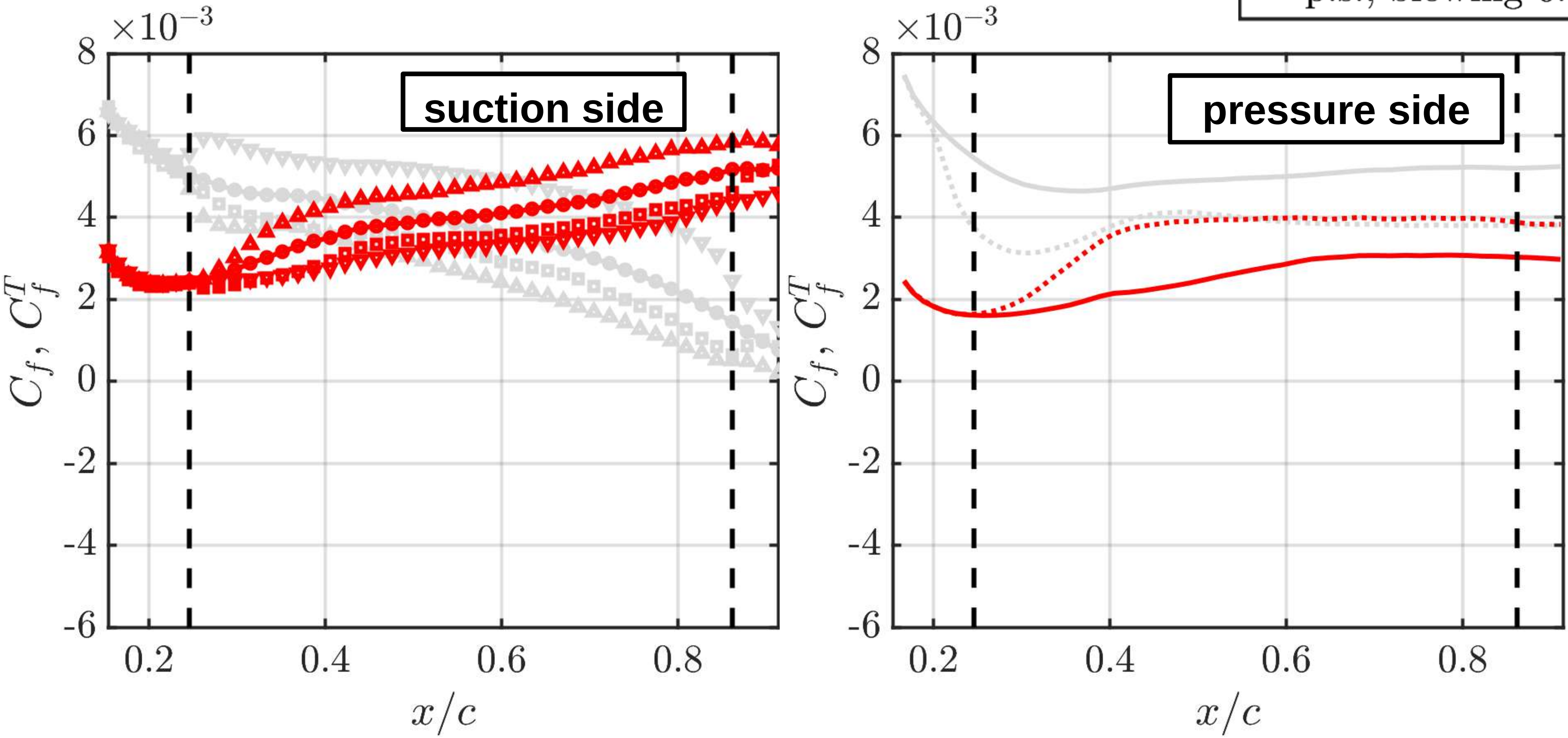

FIK: Streamwise inhomogeneity

$$I_x = \frac{\partial (U\,U)}{\partial x} + \frac{\partial \overline{uu}}{\partial x} + \frac{\partial (U\,V)}{\partial \eta} - \frac{1}{Re_\delta}\frac{\partial^2 U}{\partial x^2}$$

$$C_f^D = -2\int_0^1 (1-\eta)^2 I_x \mathrm{d}\eta$$

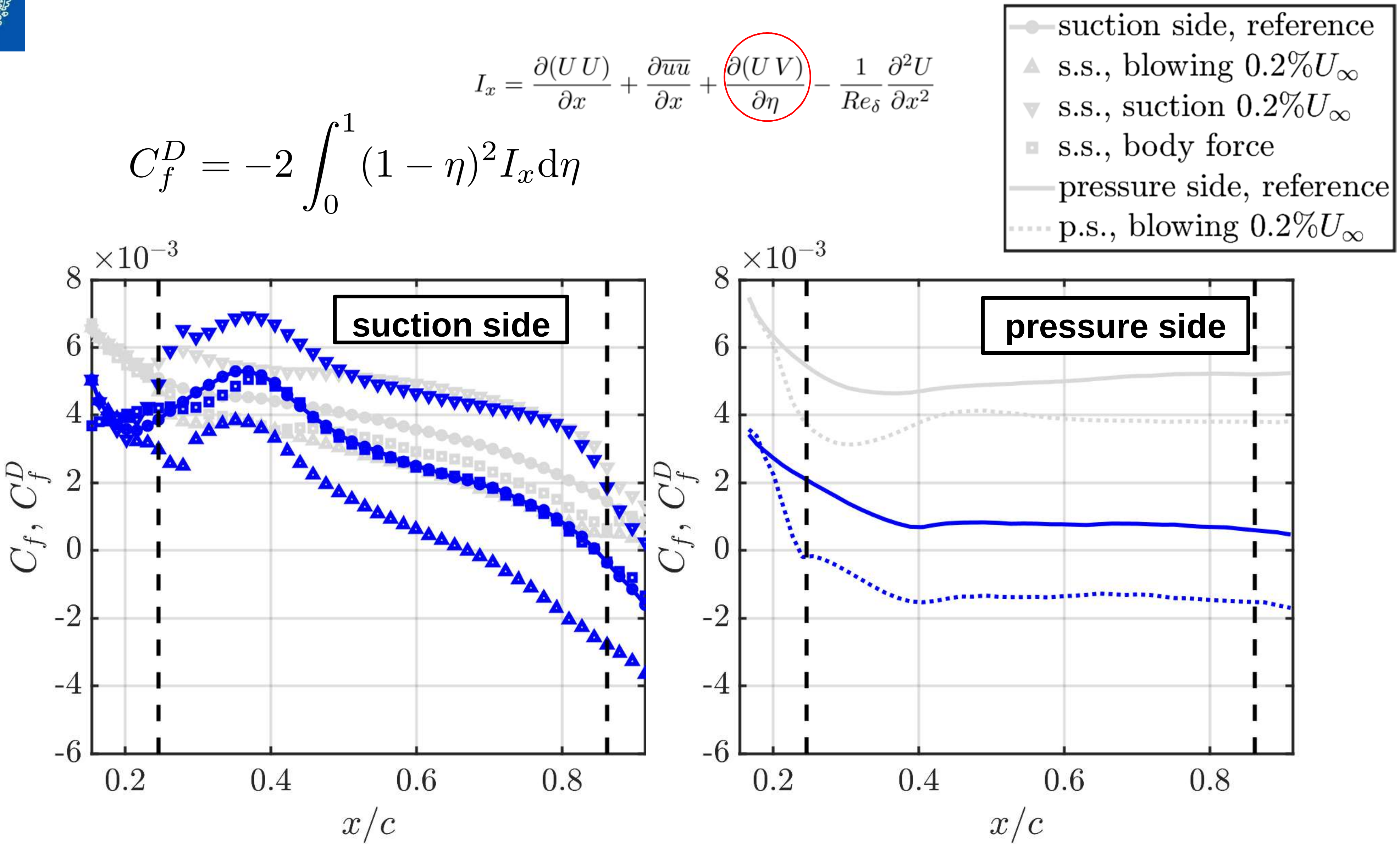

FIK: Pressure gradient

$$C_f^P = -2\int_0^1 (1-\eta)^2 \frac{\partial P}{\partial x} \mathrm{d}\eta$$

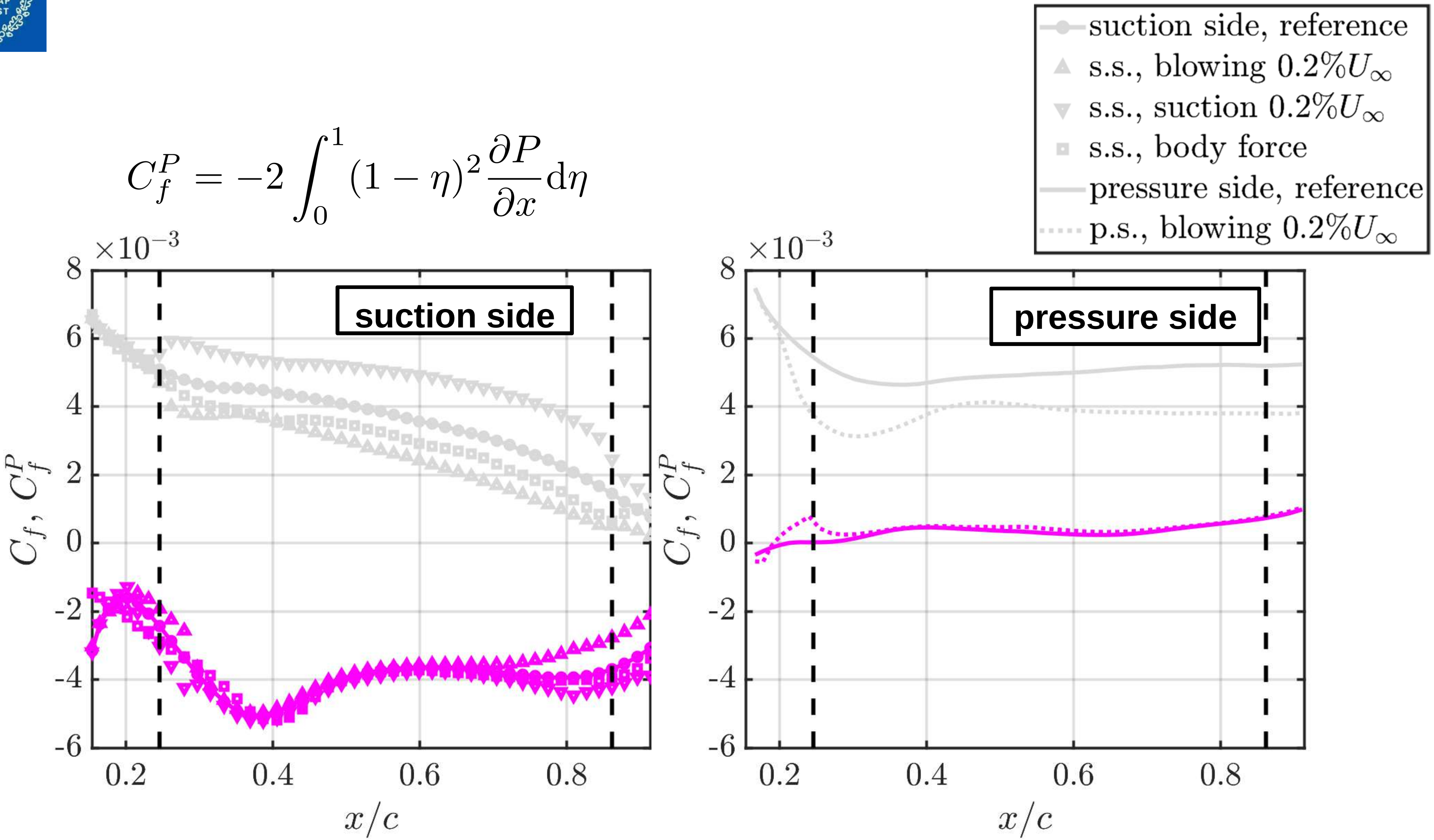

Aerodynamic effects

$$\mathbf{C_d} = \frac{\vec{F}\cdot\overrightarrow{e_x}}{\frac{1}{2}\rho U_\infty^2 c} = C_{d,f} + C_{d,p} \quad , \quad \boldsymbol{C_l} = \frac{\vec{F}\cdot\overrightarrow{e_y}}{\frac{1}{2}\rho U_\infty^2 c}$$

Case	$C_{d,f}$	$C_{d,p}$	$C_d=c_{d,f}+c_{d,p}$	C_l	L/D
Reference	**0.0125**	**0.0071**	**0.0196**	**0.87**	**44**
Blowing 0.1%, s. side					
Blowing 0.2%, s. side					
Suction 0.1%, s. side					
Suction 0.2%, s. side					
Body force 0.1%, s. side					
Blowing 0.1%, p. side					
Blowing 0.2%, p. side					

Aerodynamic effects

$$\mathbf{C_d} = \frac{\vec{F} \cdot \vec{e_x}}{\frac{1}{2}\rho U_\infty^2 c} = C_{d,f} + C_{d,p} \quad , \quad \boldsymbol{C_l} = \frac{\vec{F} \cdot \vec{e_y}}{\frac{1}{2}\rho U_\infty^2 c}$$

Case	$C_{d,f}$	$C_{d,p}$	$C_d = c_{d,f} + c_{d,p}$	C_l	L/D
Reference	**0.0125**	**0.0071**	**0.0196**	**0.87**	**44**
Blowing 0.1%, s. side	**0.0119 ↓**	**0.0082 ↑**	**0.0201 ↑**	**0.84 ↓**	**42 (-4%) ↓**
Blowing 0.2%, s. side	**0.0115 ↓**	**0.0091 ↑**	**0.0206 ↑**	**0.82 ↓**	**40 (-9%) ↓**
Suction 0.1%, s. side					
Suction 0.2%, s. side					
Body force 0.1%, s. side					
Blowing 0.1%, p. side					
Blowing 0.2%, p. side					

Aerodynamic effects

$$\mathbf{C_d} = \frac{\vec{F} \cdot \overrightarrow{e_x}}{\frac{1}{2}\rho U_\infty^2 c} = C_{d,f} + C_{d,p} \quad , \quad \boldsymbol{C_l} = \frac{\vec{F} \cdot \overrightarrow{e_y}}{\frac{1}{2}\rho U_\infty^2 c}$$

Case	$C_{d,f}$	$C_{d,p}$	$C_d=c_{d,f}+c_{d,p}$	C_l	$E=L/D$
Reference	0.0125	0.0071	0.0196	0.87	44
Blowing 0.1%, s. side	0.0119 ↓	0.0082 ↑	0.0201 ↑	0.84 ↓	42 (-4%) ↓
Blowing 0.2%, s. side	0.0115 ↓	0.0091 ↑	0.0206 ↑	0.82 ↓	40 (-9%) ↓
Suction 0.1%, s. side	0.0131 ↑	0.0063 ↓	0.0194 ↓	0.89 ↑	46 (+4%) ↑
Suction 0.2%, s. side	0.0137 ↑	0.0058 ↓	0.0195 ↓	0.91 ↑	47 (+7%) ↑
Body force 0.1%, s. side	0.0118 ↓	0.0077 ↑	0.0196 =	0.88 ↑	45 (+2%) ↑
Blowing 0.1%, p. side	0.0120 ↓	0.0070 ↓	0.0190 ↓	0.87 =	46 (+4%) ↑
Blowing 0.2%, p. side	0.0116 ↓	0.0070 ↓	0.0186 ↓	0.88 ↑	47 (+7%) ↑

Reynolds number dependency

- Friction drag becomes more relevant at higher Re
    - Optimal control mechanism expected to change

$$\delta\Phi = \Phi/\Phi_{ref}$$

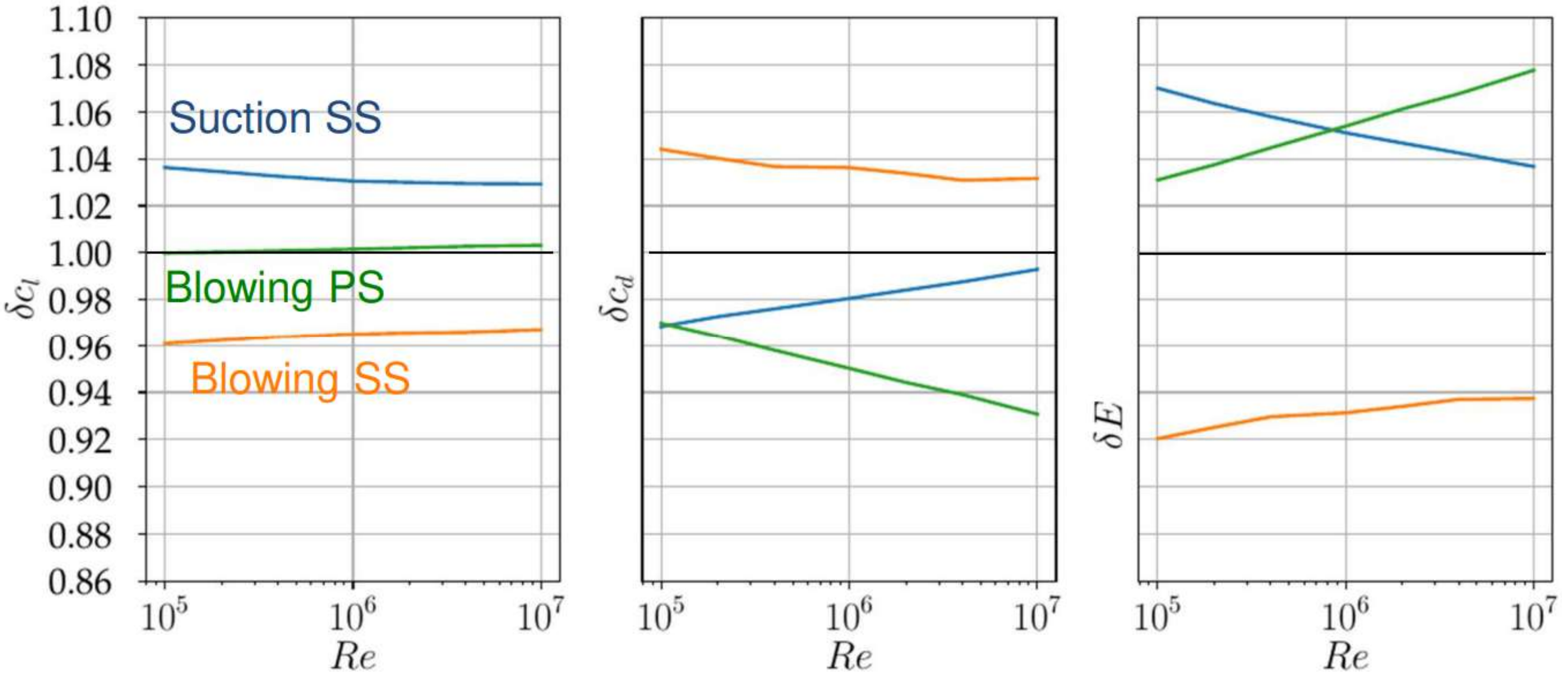

(1): Fahland, Master's thesis KIT (2019)

Reynolds number dependency

- Friction drag becomes more relevant at higher Re
  - Optimal control mechanism expected to change
  - Simulations much more expensive ($N \propto Re_c^{13/7}$ (1))

- Need an **optimized** numerical setup!

(1): Choi and Moin, Physics of Fluids (2012), 24:011702

Direct numerical simulation of flow over a full NACA4412 wing at Re_c = 400 000

- DNS with Nek5000
- Re_τ=400, Re_θ=2800
- AoA=5 deg.
- z_L=10% chord

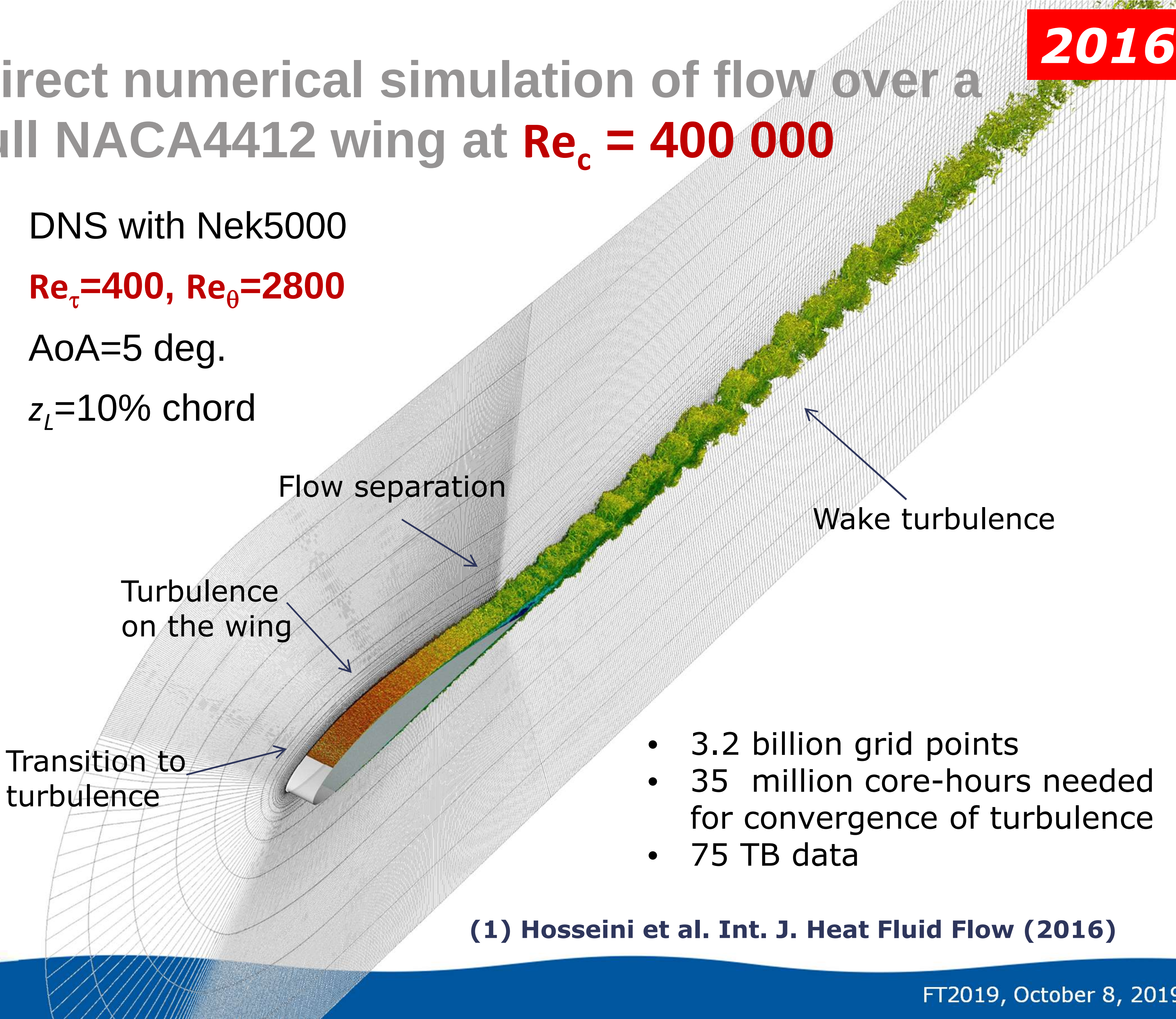

- 3.2 billion grid points
- 35 million core-hours needed for convergence of turbulence
- 75 TB data

(1) Hosseini et al. Int. J. Heat Fluid Flow (2016)

High-resolution LES of NACA-4412[1]

2018…

Factor 40 reduction in computational effort

LES with relaxation filtering (Schlatter *et al.* 2005)

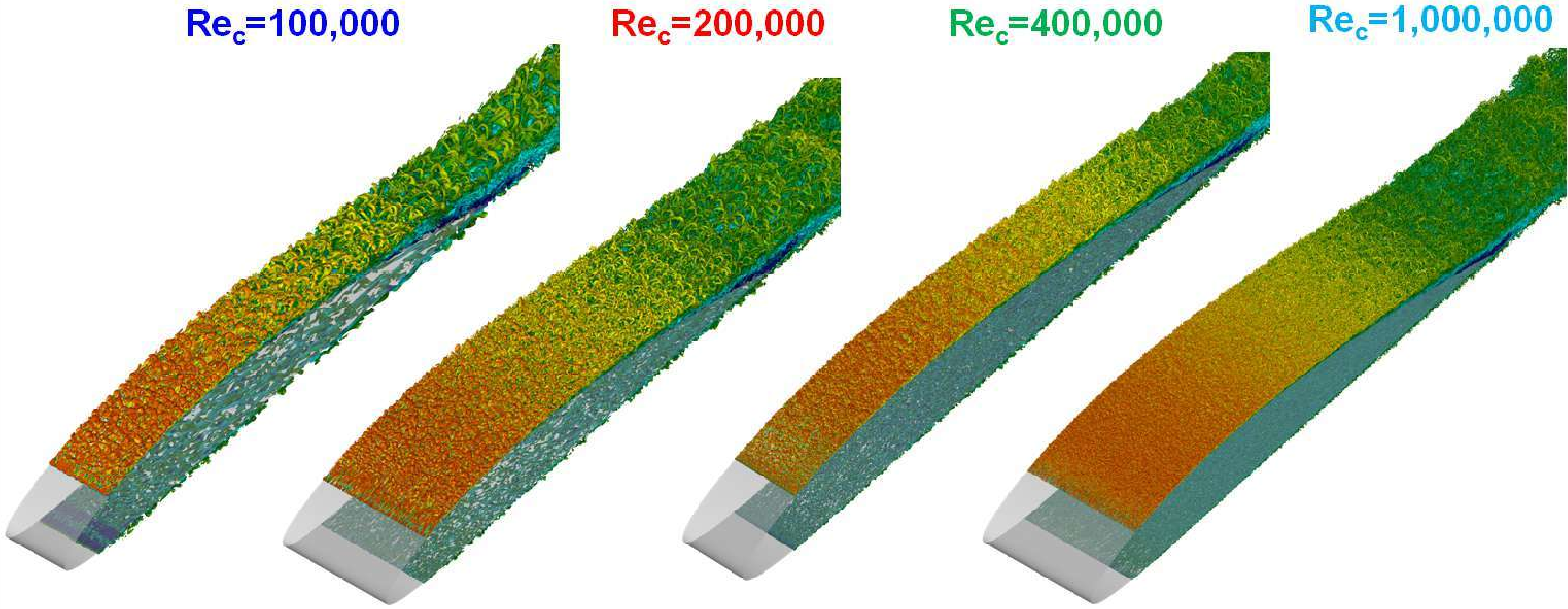

(1) Vinuesa et al. Int. J. Heat Fluid Flow 2018

High-resolution LES of NACA-4412

LES with relaxation filtering (Schlatter *et al.* 2005)

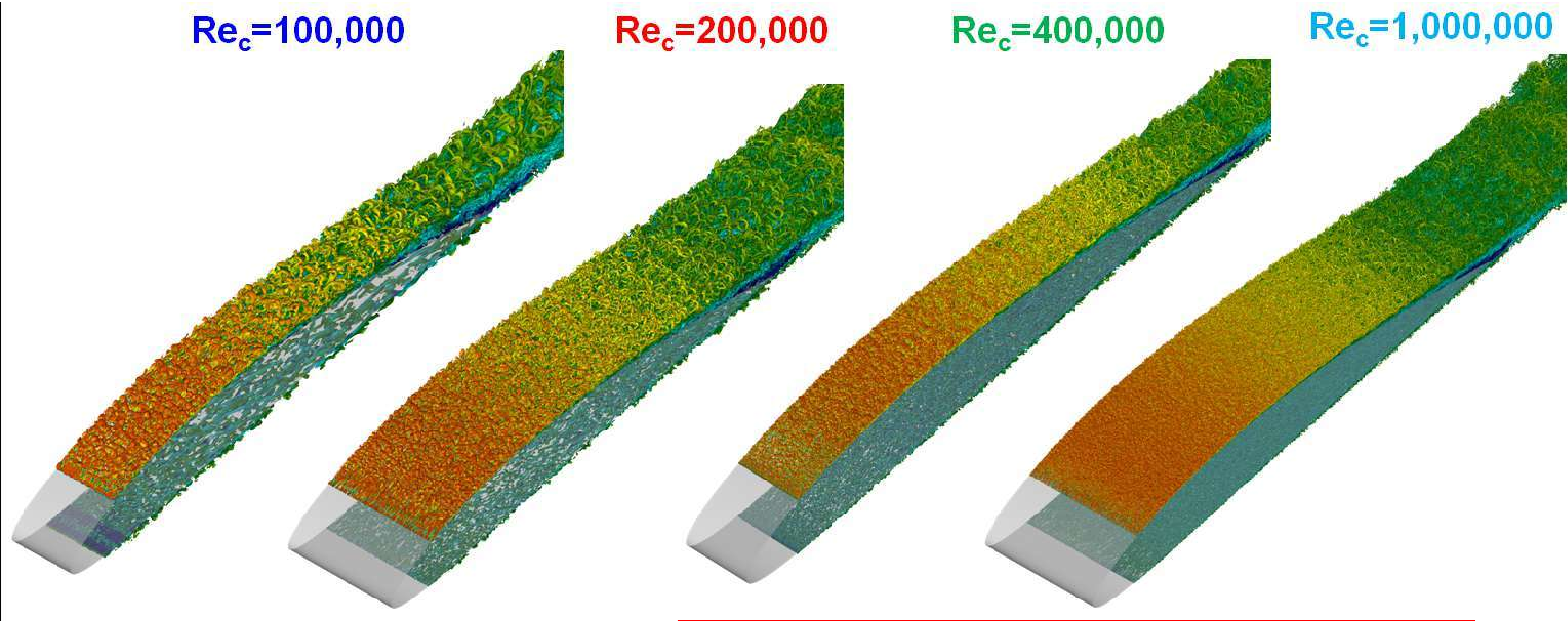

Goal: Reach (at least) **Re$_c$=1.6 M** similar to the (reference) experiments by Wadcock (1987)

Mesh refinement

Spectral grid

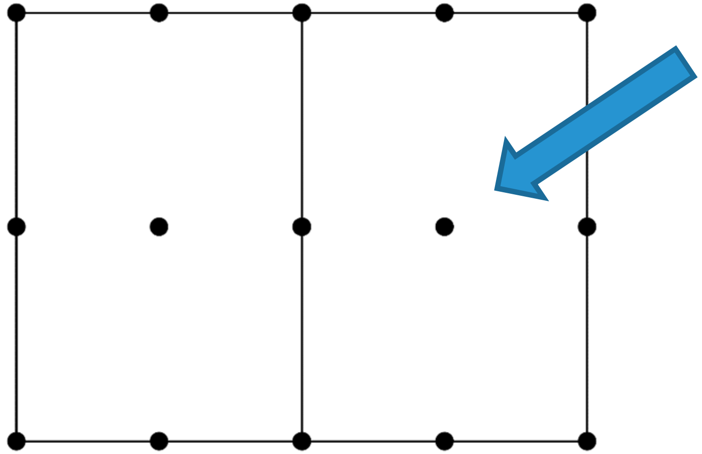

Element identified for refinement

r-refinement

p-refinement

h-refinement

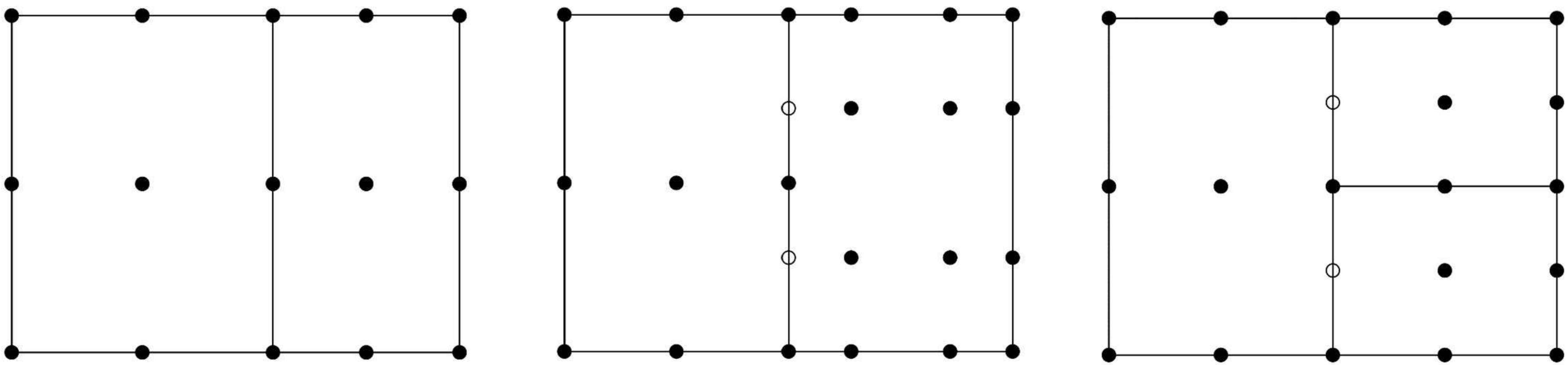

Mesh refinement

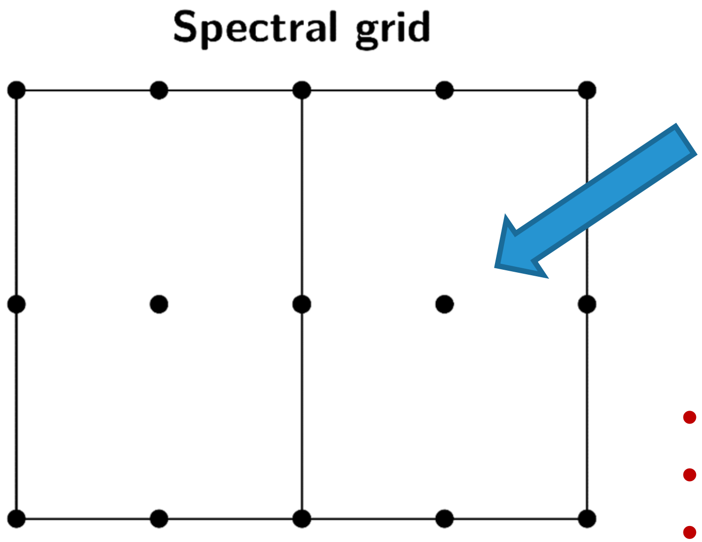

Element identified for refinement

- “Ease” of implementation
- Greatest potential
- New data structure

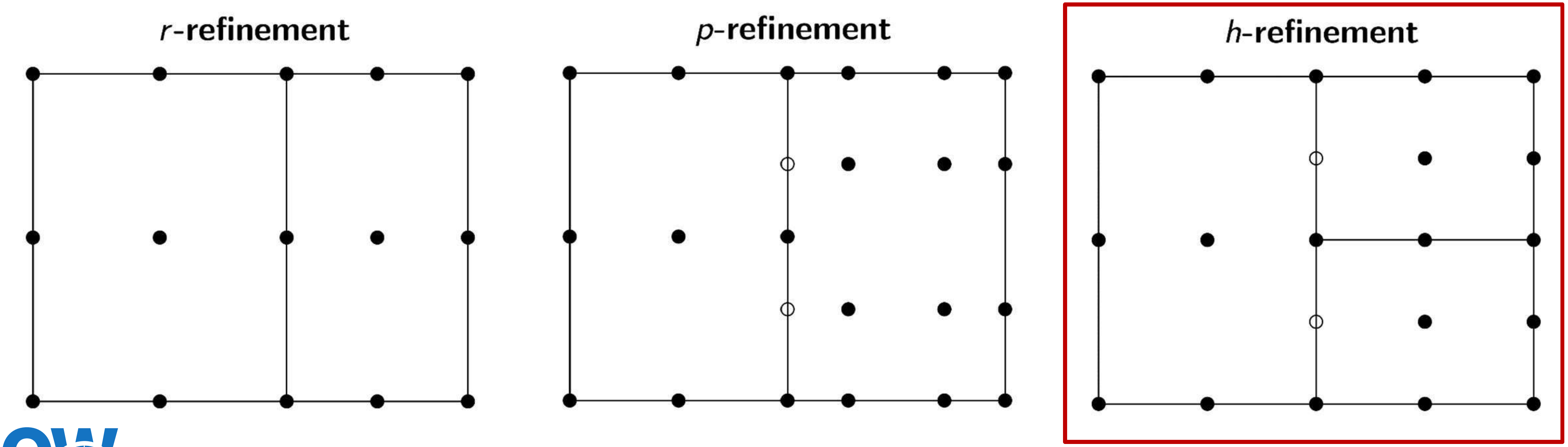

Spectral error indicator

- **Truncated spectral expansion in Legendre base in 1D (local)**

$$u(x) = \sum_{k=0}^{N} \hat{u}_k \, p_k(x)$$

$$\hat{u}_k = \frac{1}{\gamma_k} \int_{-1}^{1} w(x) u(x) p_k(x) \mathrm{d}x$$

- **Error estimate**
  - Assumed spectral decay

$$\hat{u}(k) \approx c \exp(-\sigma k)$$

  - Truncation and quadrature errors

$$\varepsilon_{\text{est}} = \left(\int_N^{\infty} \frac{\hat{u}(k)^2}{\frac{2k+1}{2}} \mathrm{d}k + \frac{\hat{u}_N^2}{\frac{2N+1}{2}} \right)^{\frac{1}{2}}$$

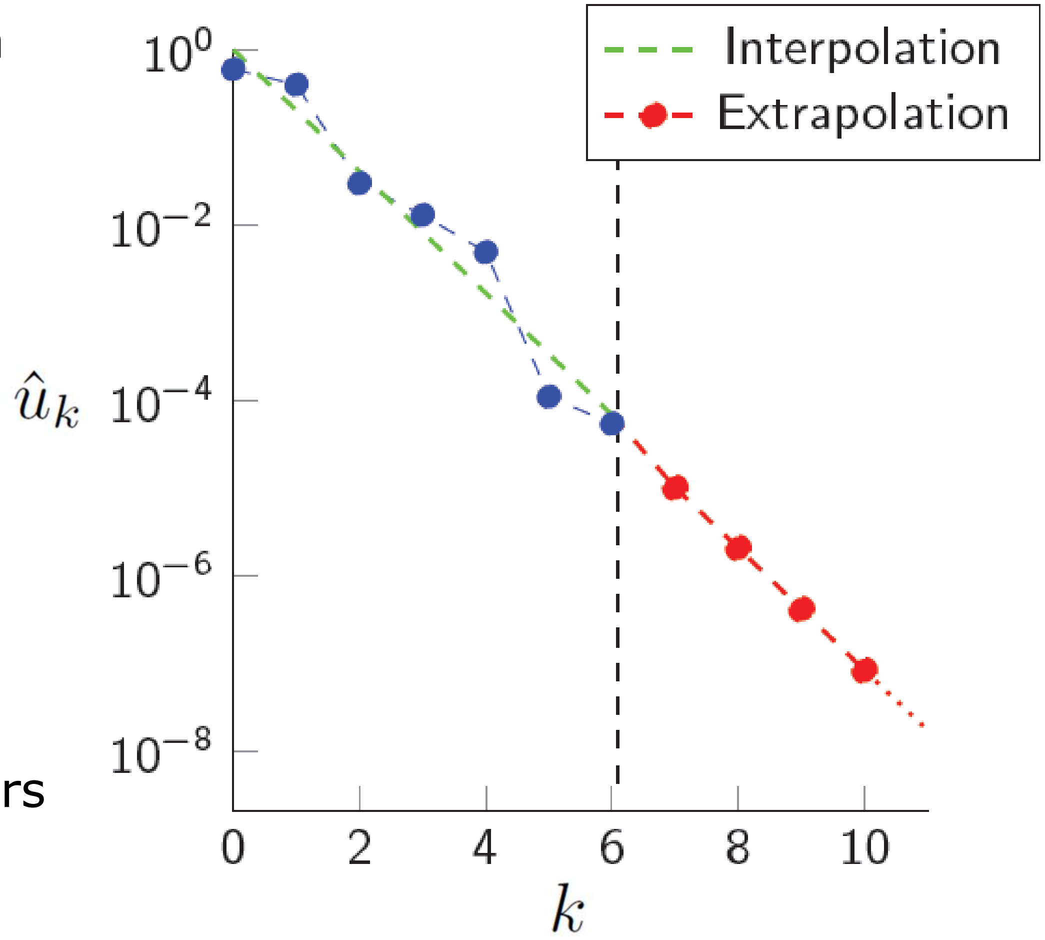

Legendre spectral coefficients

(1): Mavriplis, Comput. Methods Appl. Mech. Engrg. (1994)

Adaptive simulations with Nek5000

What we can do…

- **Fully on the fly!**
- Refining and coarsening
- Tracking features

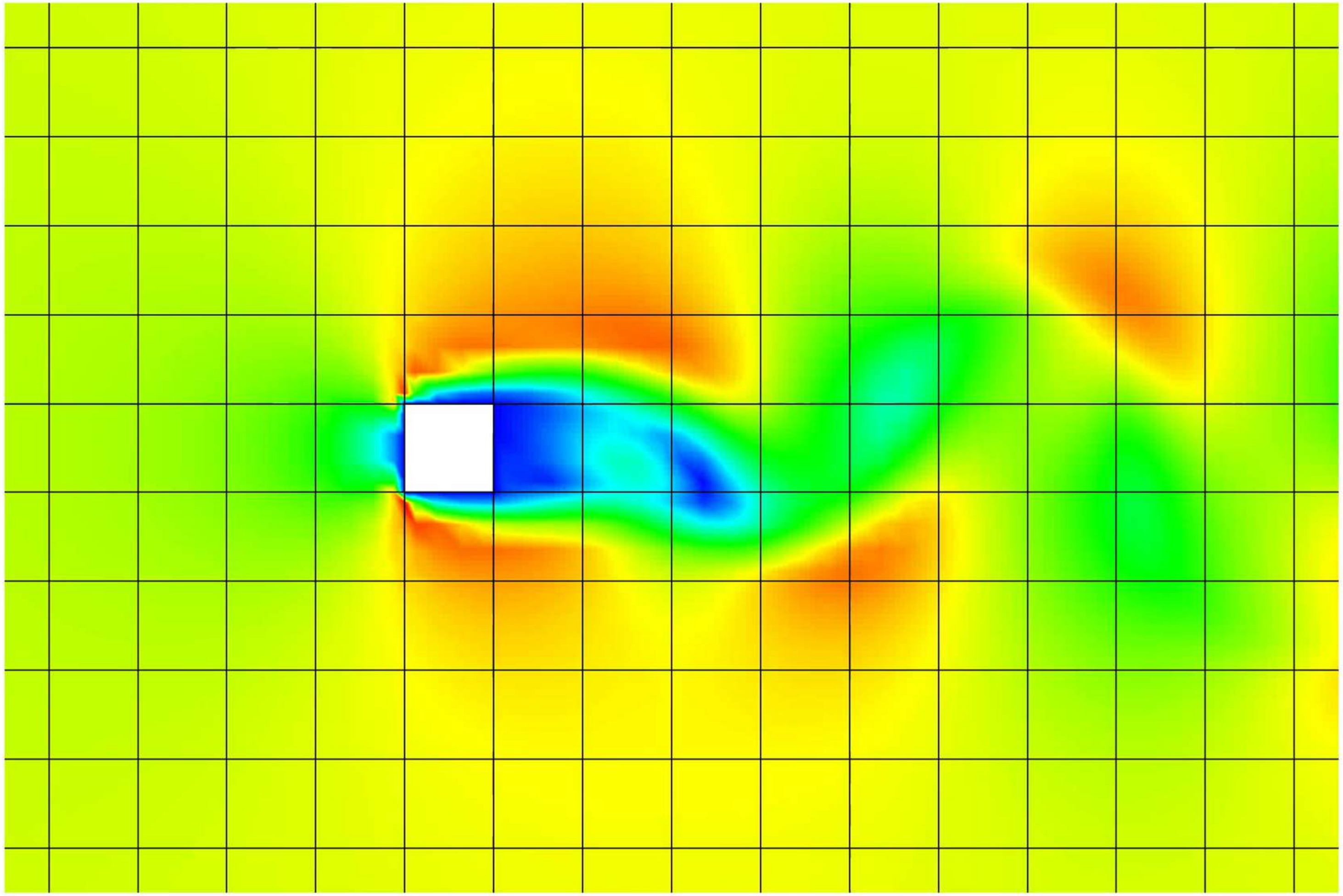

… but potentially expensive with certain error estimators!
→ *Freeze* the mesh after a run of refinements

(1): Offermans, PhD thesis KTH (2019)

3D AMR NACA 4412 Re_c = 850 000

2019

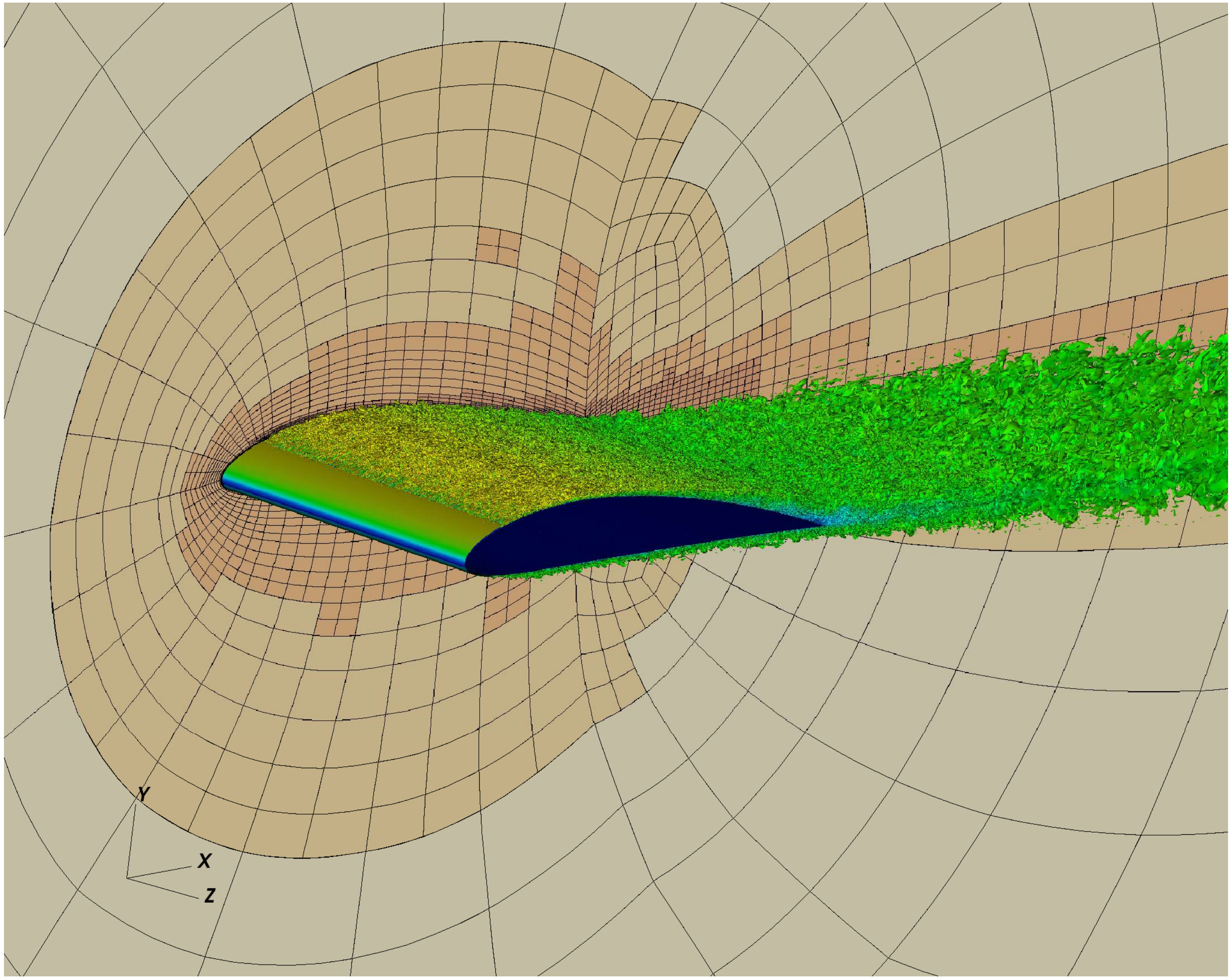

(1): Tanarro et al: TSFP 11 (2019)

Comparison between conformal and non-conformal mesh

	Conformal	Non-conformal
Code	Nek5000	
Re_c	200,000	
Resolution (wing)	**$\Delta x^+ = 18$**, $\Delta y^+ = 0.64$, **$\Delta z^+ = 9$**	**$\Delta x^+ = 7$**, $\Delta y^+ = 0.58$, **$\Delta z^+ = 4$**
Resolution (wake)	$\Delta x < 9\eta$	$(\Delta x \Delta y \Delta z)^{1/3} < 9\eta$
Domain size	$L_x = 6c$, $L_y = 4c$, **$L_z = 0.2c$**	$L_x = 40c$, $L_y = 40c$, **$L_z = 0.6c$**
Polynomial order	11	7
Number of grid points	**218 M**	**234 M** (3x larger L_z!)
B.C. inflow & top/bottom	Dirichlet (RANS)	Dirichlet $U_\infty = 1$ & Normal outflow with tangential $U_\infty = 1$
B.C. outflow	Stabilised outflow by Dong *et al.* (2014)	
B.C. in z-direction	Periodic	

AMR NACA 4412, Re_c = 200 000

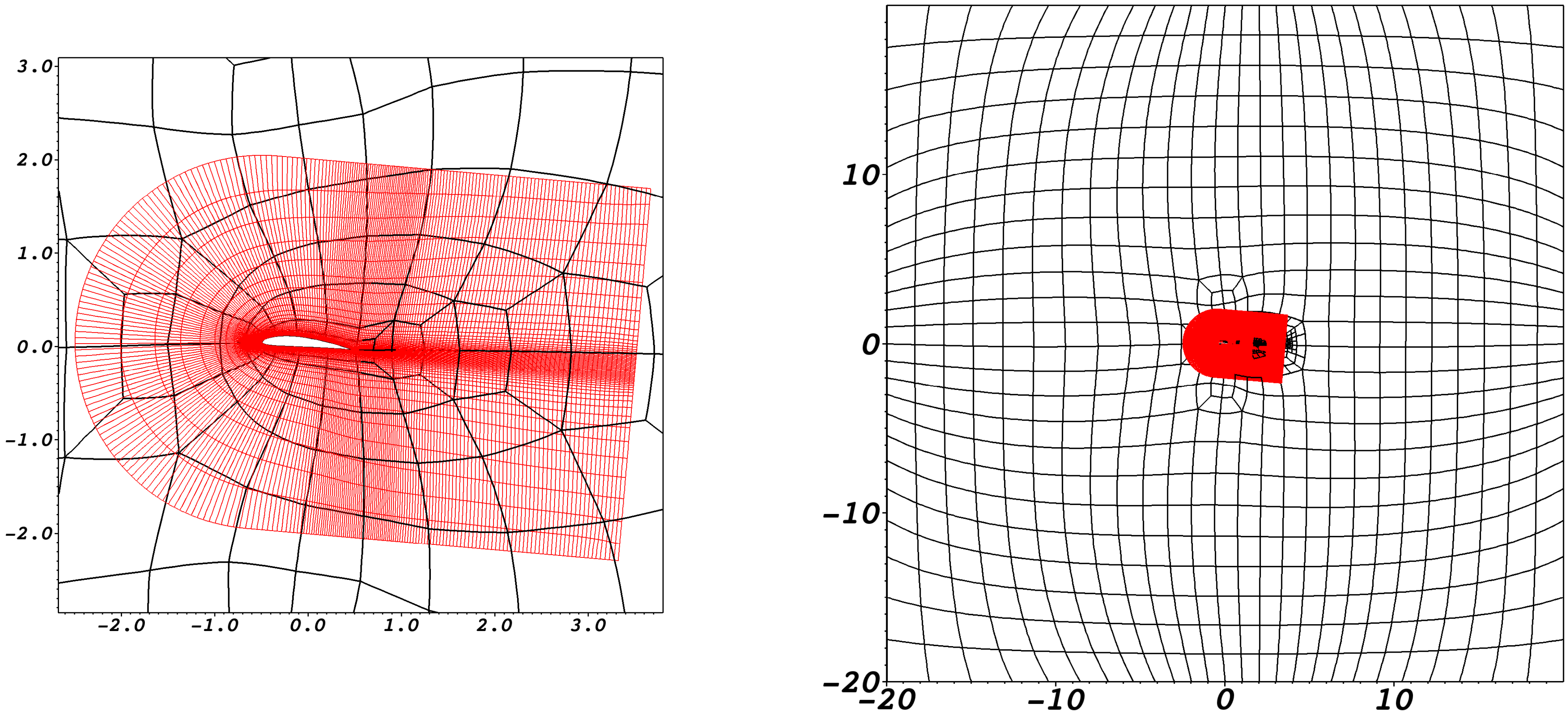

Comparison of mesh structure

Skin-friction coefficient and 99% boundary layer thickness (Re_c=200k)

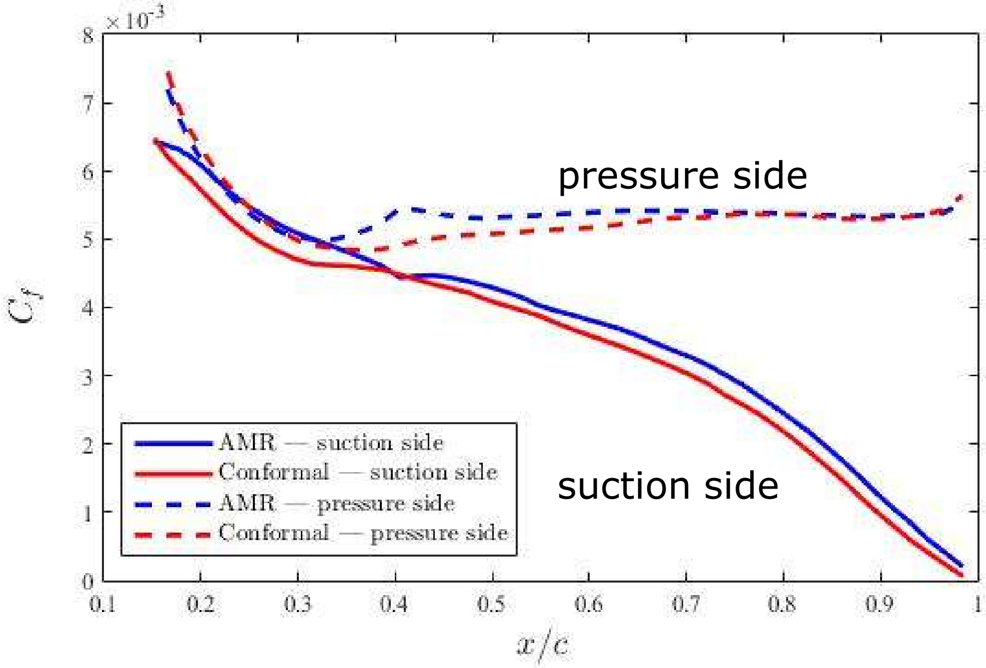

Slight discrepancy in the skin-friction coefficient which could be the result of the higher resolution of the non-conformal mesh in the wall.

Excellent agreement on the computation of the boundary-layer thickness δ_{99}.

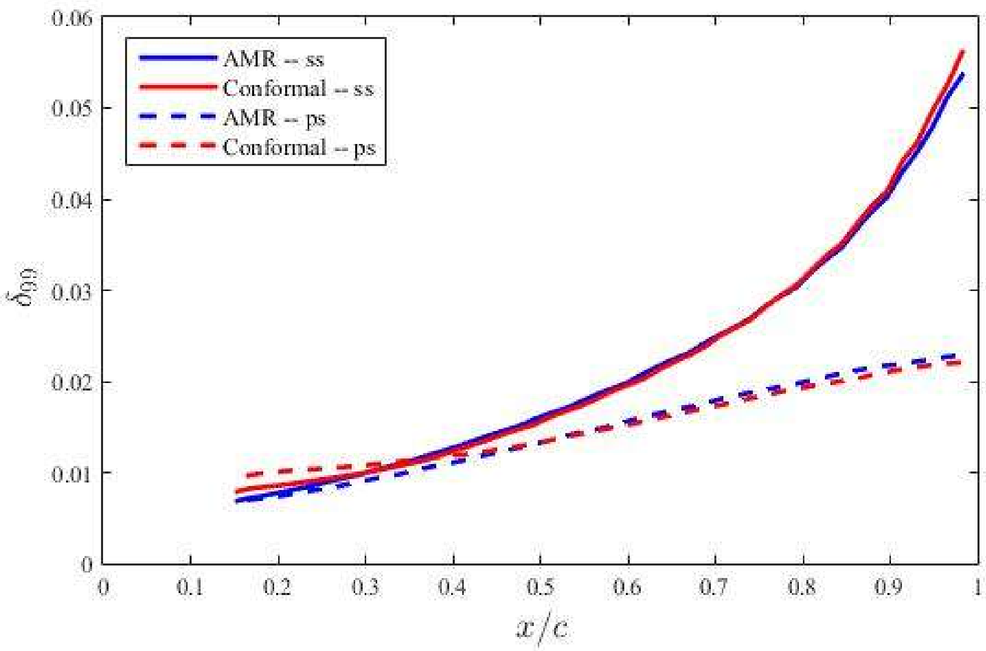

Mean velocity and rms profiles (Re_c=200k)

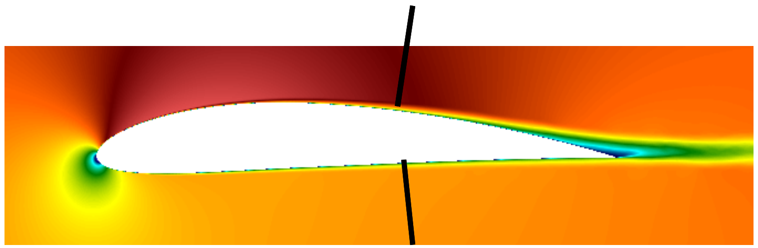

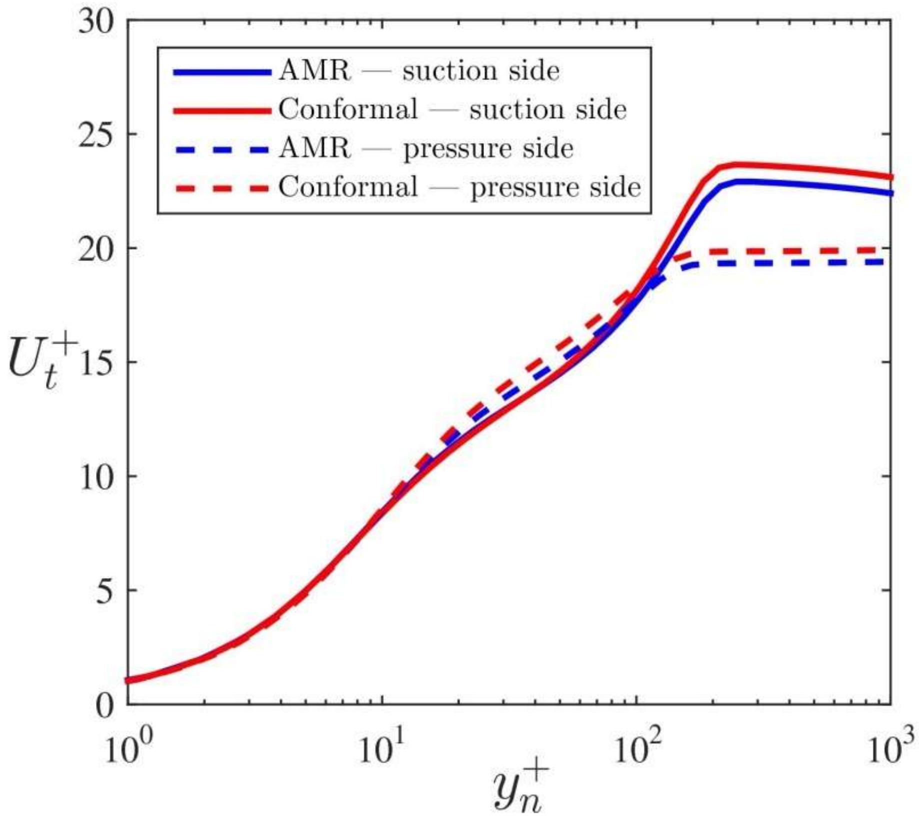

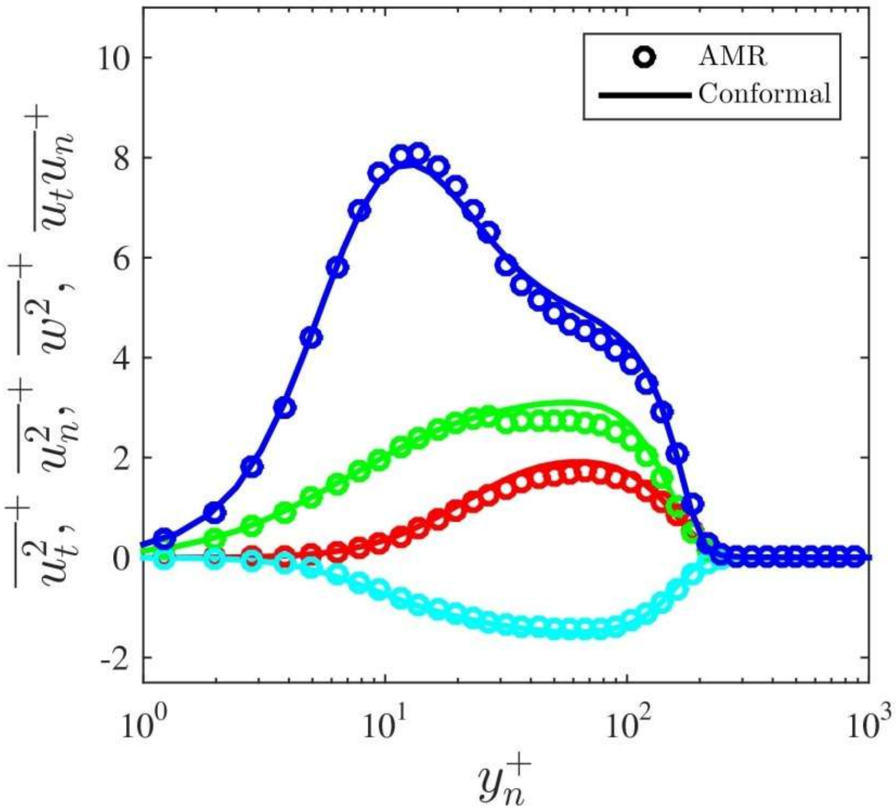

Differences are mostly due to inner scaling (i.e. the friction coefficient). All the qualitative aspects are recovered with both simulations.

“Real Experiments” in the MTL wind tunnel (KTH Mechanics)

- Complement and extend numerical simulations
- Reynolds number up to 2 M

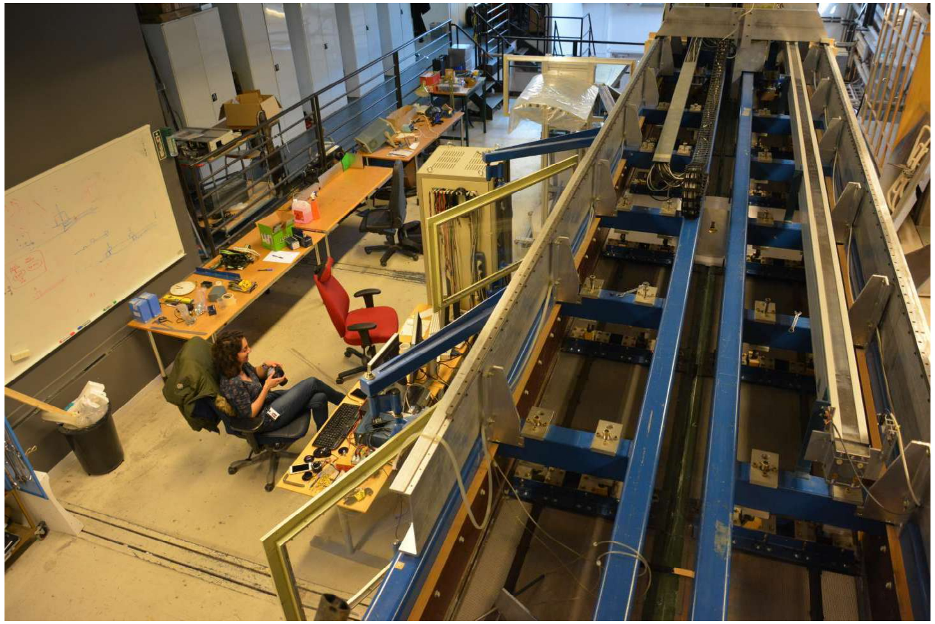

Spring 2019: Implementation and validation

“Real Experiments” in the MTL wind tunnel (KTH Mechanics)

- Complement and extend numerical simulations
- Reynolds number up to 2 M

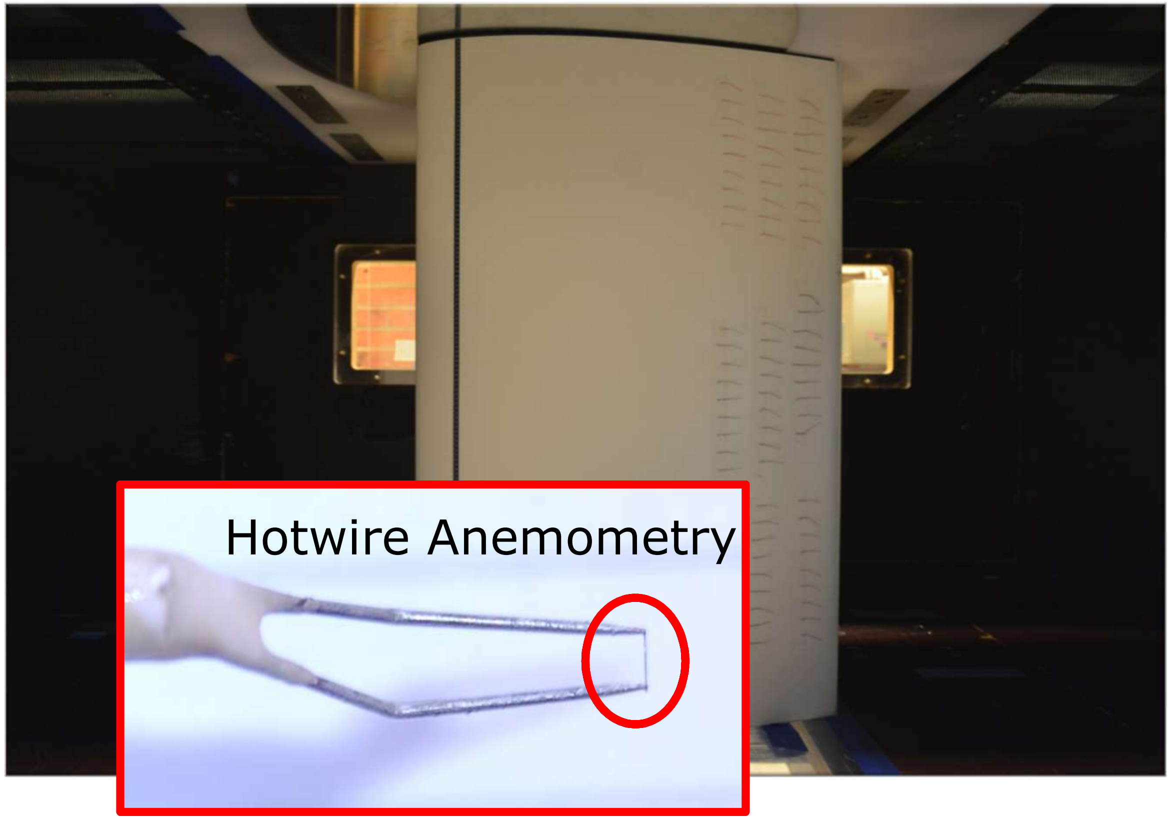

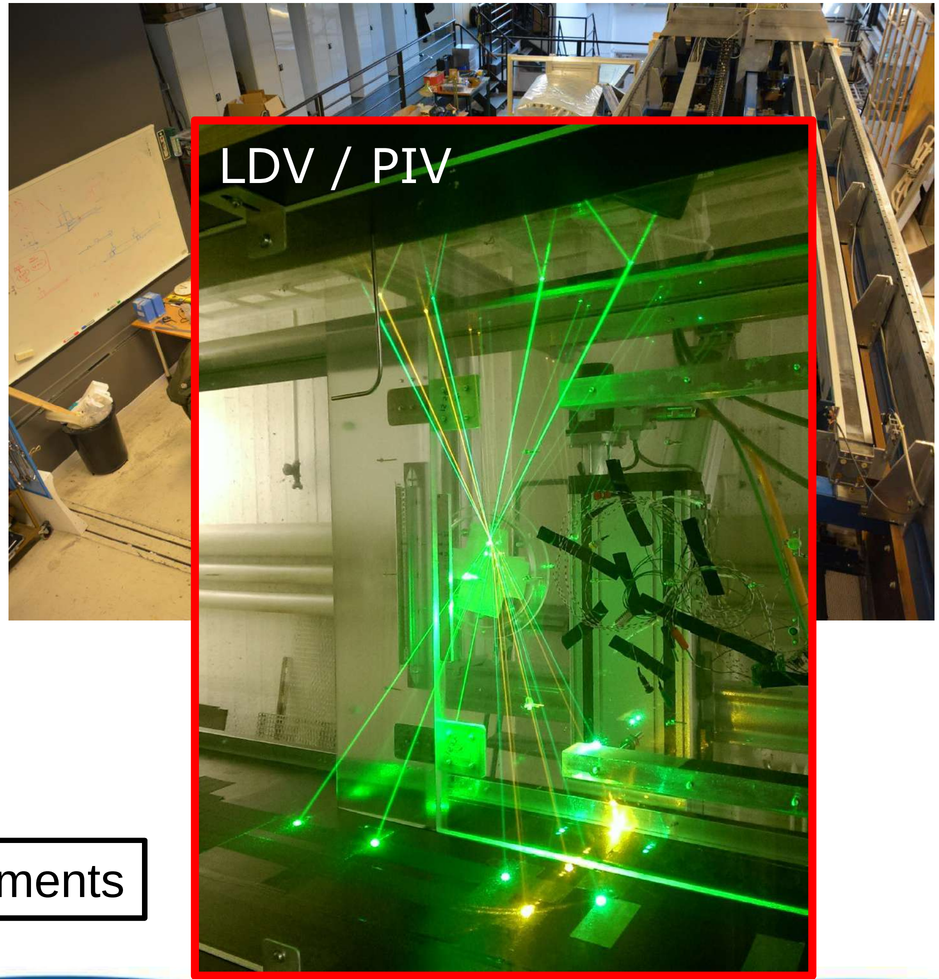

Spring 2020: BL measurements

LINNÉ FLOW CENTRE

Conclusions

- Flow-control simulations using **high-order (spectral) methods**
- First in-detail study of the different contributors to drag on a wing
- Suction on suction-side and blowing in pressure-side lead to highest drag reduction at moderate *Re*
- Steps towards increasing the achievable *Re*
    - LES RT-filtering
    - Implementation of **Adaptive Mesh Refinement** (AMR) in NEK5000
- Highest *Re* for reference high-fidelity data of turbulence in wings
- Experiments in the MTL wind tunnel

Knut och Alice Wallenbergs Stiftelse

FLOW LINNÉ FLOW CENTRE